Development of Methods to Study Synthetic Histones *In Cellulo*

Undergraduate Research Thesis

Presented in partial fulfillment of the requirements for graduation *with honors research distinction* in Biochemistry in the undergraduate colleges of The Ohio State University

by
Angela Harrison

The Ohio State University
May 2015

Project Advisor: Professor Jennifer Ottesen, Department of Chemistry and Biochemistry

TABLE OF CONTENTS

List of figures

Number **Page**

Acknowledgements

I would first like to thank Dr. Jennifer Ottesen for getting me involved in undergraduate research and serving as a teacher and mentor. Her support and guidance have shaped me as a scientist. She has pushed me to achieve things I never thought I could.

I also must thank CJ Howard for all of his guidance. He transformed me from a new, clueless lab member into an independent researcher who can plan and execute experiments as well as pass my knowledge along to others. He has taught me all the skills I have learned here.

Thank you to Dr. John Shimko for our chats which give me breaks from work. A big thanks to Sarah Dreher for bringing cookies. Thanks to Mitchell Weeman for letting me attempt to teach him everything I've learned here over the past two years.

This work was partially supported by a Mayers Summer Research Scholarship to ACH, and by NSF grant MCB-0845695 to JJO.

Abstract

Post-translational modifications of histone proteins are essential to the regulation of chromatin structure and DNA accessibility in the eukaryotic cell. The ability to prepare synthetic, chemically-modified histone proteins has enabled fundamental insights into the functions of histone post-translational modifications. However, these powerful chemical approaches inherently limit studies to an *in vitro* context which lacks the complexity of native biological systems. Here we develop tools to introduce exogenous, chemically-synthesized histones into different eukaryotic cell lines for assembly into chromatin in the cell nucleus.

Previous studies have demonstrated successful uptake of recombinant H2A/H2B dimer and $H3_2/H4_2$ tetramer into the nuclei of *Physarum polycephalum*, a myxomycete slime mold. We repeat these results and extend them to show uptake of histones into a common air-borne mold of the *Mucor* genus, rat IEC cells, and human breast cancer MDA-231 cells. We demonstrate nuclear import of exogenous fluorescently-labeled histones into multiple cell lines through gel electrophoresis of isolated nuclei. Preliminary fluorescent microscopy experiments support the colocalization of DNA and fluorescently-labeled exogenous histones in live and in fixed cells. Avidin pull-downs of intact nucleosomes after uptake of biotin-labeled histone dimer indicate incorporation of these histones into chromatin. Our results suggest that certain histone proteins display cell penetrating characteristics, which may provide a method for the study of homogenous semi- or fully-synthetic chemically-modified histones within the complex systems of eukaryotic cells.

Chapter 1: Introduction

Eukaryotic DNA is organized into chromatin in the nucleus. The basic unit of chromatin is the nucleosome, composed of ~147 bp of DNA wrapped around a protein core of histones. This core consists of two copies each of H2A, H2B, H3, and H4 (**Fig. 1**). The structure of the nucleosome regulates chromatin structure and DNA accessibility and therefore plays an important role in DNA transcription, translation, and replication. Nucleosome structure is regulated in part by post-translational modifications (PTMs) to histone proteins that alter interactions between histones and DNA as well as between the histones themselves, causing a multitude of changes such as loss of DNA-histone affinity and instability of the nucleosome core (1).

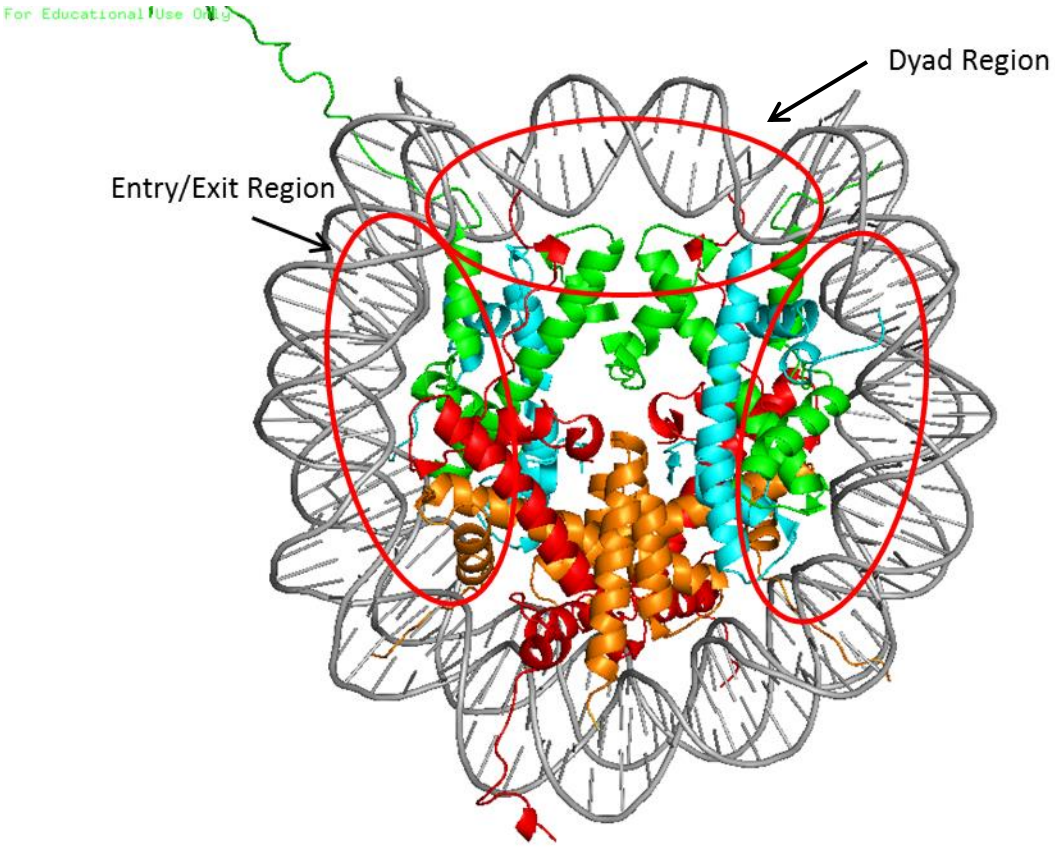

Figure 1. Structure of the nucleosome. Red: H2A, Orange: H2B, Green; H3, Blue; H4, Gray: DNA. The entry/exit and dyad regions are labeled.

Histone Modifications

Many different types of histone modifications have been found in nature, including phosphorylation, methylation, and acetylation. The function of each modification depends heavily upon where it is in the nucleosome. PTMs in the histone core (see **Fig. 1**) alter histone-histone interactions that often destabilize the nucleosome. This can cause the nucleosome to unfold and increase the potential of first the H2A/H2B dimers and then the H3/H4 tetramer to dissociate from the DNA (2). Modifications in the entry/exit region can regulate wrapping and unwrapping of DNA around the nucleosome and therefore can allow partial access to the DNA which is important for the removal or shifting of core histone proteins (3). PTMs in the dyad region alter histone-DNA affinity as well and influence nucleosome sliding, a process that does not disassemble the nucleosome but rather slides the core histones along the DNA (3, 4). PTMs can further regulate the cell's function by modulating interactions with other types of proteins such as transcription factors or polymerases by serving as platforms for binding (5).

Sets of modifications tend to appear in context-dependent patterns, leading to the hypothesis that each modification or group of modifications has a function that helps to modulate the local environment around the modifications to specifically regulate DNA processes (6). DNA-related and histone-modifying enzymes show specificity for certain types of modifications to specific histone residues (5). Also, isolated histones tend to contain conserved sets of modifications. For example, serine 1 of histone H4 is generally acetylated. In newly-synthesized H4, lysines 5 and 12 in the N-terminal tail are acetylated. These acetylations have been further connected to acetylation at lysine 91 in the histone-chaperone complex that deposits histone proteins into chromatin (7).

Studying Post-translational Modifications

The study of modified histones poses an interesting problem since it requires homogeneously-modified proteins. *In vivo*, enzymes such as histone acetyltransferases, deacetylases, phosphatases, methyltransferases specifically modify histone proteins (6, 8); however, use of these enzymes to modify histones *in vitro* presents multiple problems. While histone-modifying enzymes appear to act with some specificity in a cellular environment, this same site specificity is often lacking *in vitro*. This lack of specificity results not only in modifications at undesirable sites but in a failure to control the extent of modification (9). Furthermore, modifying enzymes have been studied to different extents, and a full set of isolated enzymes that can create all sets of modifications does not exist (10).

Some recombinant modified histones can be expressed through amber codon suppression or with modification mimics, but these techniques are limited. First of all, expression by amber codon suppression requires significant bioengineering such as the creation of transgenic cell lines that will encode non-natural tRNAs and amino acid tRNA synthetases. Successful amber codon expression has been shown in eukaryotic cells, including mammalian cultures (11, 12), but the bulk of this expression is accomplished in prokaryotic systems, which do not have histones. Expression of the mutant proteins also results in smaller yields than are observed with the wild type variants, especially when multiple amber codon sites are used (13). Lastly, many modifications are currently outside the scope of amber codon suppression. Successful incorporation of acetyllysine, methylhistidine, and other non-canonical amino acids into proteins has been demonstrated in *E. coli* (13, 14). Incorporation of mimics for modifications such as acetyllysine and methyllysine has also been shown (8); however, many modifications such as ubiquitination, which adds an entire protein to the histone, cannot be incorporated using this

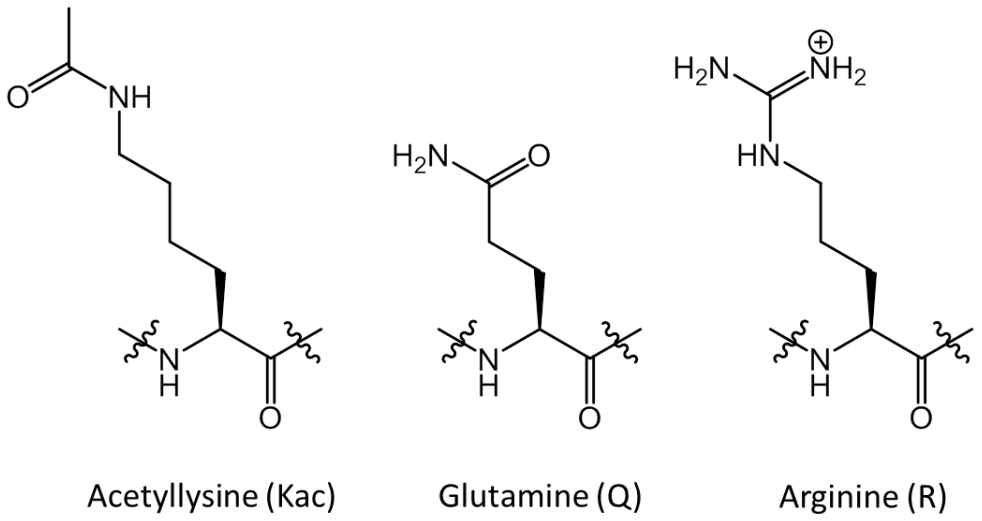

Figure 2. Common acetyllysine mimics. Both glutamate and arginine have been used to mimic acetyllysine with varying degrees of success.

method.

Modification mimics have been used in the past to elucidate important functions of some modifications in the cell. The advantages to mimics are that they can often be introduced recombinantly and can overcome some of the drawbacks and limitations of amber codon suppression. Modification mimics are generally able to approximate the charge, shape, or size of the modified residues, though they rarely mimic every aspect of the native modification (5, 15). For example, both glutamine and arginine have been used to mimic acetyllysine (**Fig. 2**). While glutamine is able to approximate the charge loss caused by acetylation of the positively-charged lysine residue, the steric bulk is notably different. Also, though glutamine is uncharged, the end of its side chain is polar, and the nitrogen has a partial positive charge. Arginine, on the other hand, has a similar size to acetyllysine, but retains a positive charge that the acetylation removes. Indeed, these mimics have been shown to behave differently from the native modifications (4).

Chemical Protein Synthesis

Our laboratory has pioneered in the synthesis of full-length modified histone proteins. Our main approach is chemical synthesis of modified peptides and ligation to either recombinantly-expressed protein thioesters in a process called expressed protein ligation (EPL) or to other chemically synthesized peptides via native chemical ligation (NCL) to create full-length modified histone proteins (16, 17). This strategy allows specific control of both the location and

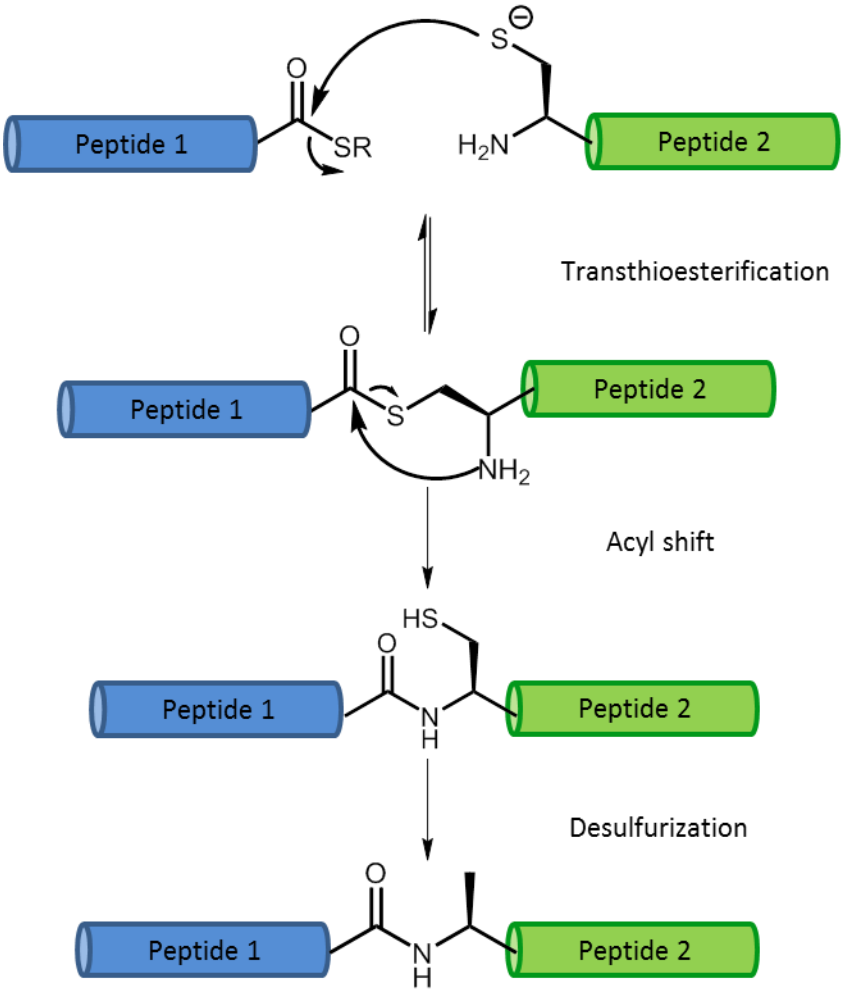

Figure 3. Schematic of ligation.

type of modification in each protein, but has typically been limited to *in vitro* study.

A schematic of ligation is illustrated in **Figure 3.** The N-terminal piece must contain a C-terminal α-thioester which can be introduced either recombinantly, through fusion with an intein in the expression plasmid and thiolysis following purification to reveal the thioester, or as part of the chemical synthesis of the peptide. The C-terminal piece must contain an N-terminal 1,2-aminothiol, generally a cysteine. During ligation, the sulfur of the cysteine will replace the thioester sulfur by attacking the carbonyl and displacing the thioester in a transthioesterification process, creating a bond between the two pieces. This then undergoes a spontaneous acyl shift from the thioester to an amide bond with the nitrogen from the N-terminus. This reaction yields a full protein made from the two segments, with a native amide bond at the ligation junction (16, 17).

Ligation sites, of course, require a cysteine; however, the histone core contains only one cysteine. In these cases, ligation sites can be chosen at alanine residues. The cysteine can be desulfurized using a radical mechanism to reveal the native alanine (18). This technique can also be used with other residues such as glutamine (19), valine (20), leucine (21), and even proline (22). In these cases, N-terminal amino acid is a thiol-modified residue with a thiol group attached at the β-carbon.

Developing Methods for *In Vivo* Study of Chemically-Modified Histones

Chemical protein synthesis is extremely powerful but limits modification studies to an *in vitro* system. While *in vitro* studies have revealed many insights into the functions of histone modifications as they relate to chromatin structure and DNA processes, these experiments lack the complexity of native biological systems. There remains the need for tools introduce

exogenous, chemically-synthesized histones into a cellular environment to observe how specifically modified histones interact with the cellular machinery and thereby gain a greater understanding of their role.

The slime mold *Physarum polycephalum* has been claimed to have a unique ability to uptake macromolecules, particularly histone proteins, from its external environment, most likely through an endocytotic or pinocytotic mechanism. Not only does this organism not break down exogenous histones, but it incorporates them into its own cellular processes (23, 24). We therefore hypothesized that *P. polycephalum*, then, may provide an opportunity to quickly and easily study synthetic proteins *in vivo*. In this thesis, we describe our progress towards this goal, and further, explore cell penetrating behavior of histones in multiple eukaryotic cells.

In order to study histones *in vivo* in a eukaryotic system, they must be distinguished in some way from the native histones, as well as made easy to visualize via our analysis methods. In Chapter 2, we discuss the techniques used for histone labeling. We introduce both fluorescent and affinity labels to histone proteins. Standard methods can be used to label histones with maleimide-functionalized labels through alkylation of cysteines introduced through well-defined site-directed mutagenesis. However, this approach is not compatible or efficient with protein semi-synthesis and desulfurization. Instead, we developed an approach in which the N-terminal serine of either H2A or H4 is converted into an aldehyde which then serves as a labeling handle. This technique is compatible with recombinant, semi- and fully-synthetic histones and allows divergent labeling of a single protein preparation. Further, we demonstrate compatibility with maleimide labeling by the generation of a dual-labeled H2A with an N-terminal biotin attached through aldehyde introduction and a fluorescein added through cysteine alkylation.

In Chapter 3, we demonstrate uptake of exogenous histones into *P. polycephalum*. We further demonstrate transport of these proteins into nuclei, and specifically into chromatin. These results allow study of chemically-synthesized modified histones to be studied in the relevant and complex environment of the eukaryotic nucleus.

In Chapter 4, we explore uptake of exogenous histones into a variety of eukaryotic cell models, based on the observation that the unstructured, positively charged tails of histone proteins resemble canonical cell penetrating peptides (25). We demonstrate histone uptake into a true mold of the Mucor genus as well as rat intestinal endothelial cells (IEC), human HeLa cells, and breast cancer MDA-231 cells. This allows histone PTMs to be studied in an increasingly relevant environment including mammalian cell lines and lays the groundwork for a better understanding of how these PTMs interact with a cellular environment and therefore of their function and cross-talk with other modifications, which can provide insights into human disease such as cancer.

Chapter 2: Chemical Labeling Strategies for Histone Proteins

Introduction

In order to track exogenous histones once they enter a cell, they must be labeled in some fashion to distinguish them from the endogenous histones of that cell line. The most common approach in the literature is introduction of maleimide-functionalized labels at cysteines introduced by site-directed mutagenesis in well-studied locations. This labeling technique works through alkylation of the side chain sulfur (see **Fig. 4**). This method is typically appropriate for nucleosomes since the only native Cys is H3-C110, which is typically removed. Common cysteine introduction sites include H2A-K119C and H3-V35C (5). Our laboratory commonly uses this approach to prepare bulk, labeled recombinant histone proteins, and several histones labeled by this approach are used throughout this work. This approach is sufficiently common that we do not include here any characterization of these molecules.

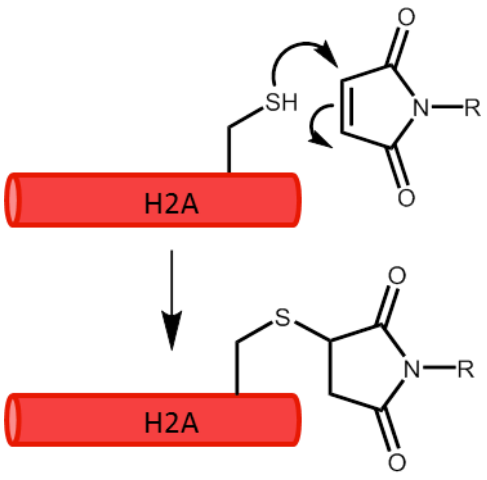

Figure 4. . Maleimide labeling schematic. R represents the label. It can be a fluorophore such as fluorescein or a pull-down tag such as biotin.

In spite of the advantages of this technique, maleimide labeling is generally unsuitable for semi- and fully-synthetic histones. The desulfurization step removes all cysteines from the protein after ligation, thereby removing the maleimide-reactive group. This problem can be overcome by synthesis of a label into one of the peptides, but this method requires production of a specific peptide and semisynthetic or fully synthetic protein for a single use. The number of required syntheses and ligations would therefore increase dramatically. Because production of synthetic proteins is costly and time-consuming, this approach is undesirable. Instead, we sought to develop a more creative labeling approach for semi- and fully-synthetic histones that is specific enough to label each protein only once, does not disrupt protein folding or interactions with other molecules, can be done under relatively gentle conditions, and which can introduce this diversity of labels into a single batch of prepared histone. We hypothesized that aldehyde labeling would provide this approach.

Histones H2A and H4 have an N-terminal serine residue which is a 1,2-aminol with a primary amine (1), a relatively unique property within the cell. Sodium periodate can oxidize these 1,2-aminols to create an N-terminal aldehyde moiety, making these proteins perfect candidates for specific labeling (schematic in **Fig. 5**). The aldehyde can be derivatized with hydroxylamine or hydrazide functionalities, forming an oxime or a hydrazone bond respectively. This bond can then be reduced with $NaBH_4$ to create an irreversible linkage between the label and the aldehyde-converted molecule. (26, 27). Labeling using this technique allows wild type recombinant H2A and H4 to be labeled easily, and is further compatible with a semi-synthetic or fully-synthetic strategy for histone production. The ability to label both of these proteins using this method provides a means of introducing a label into both histone dimer and histone tetramer, the two

complexes that make up the histone core of the nucleosome, allowing us to independently probe the relevant histone complexes.

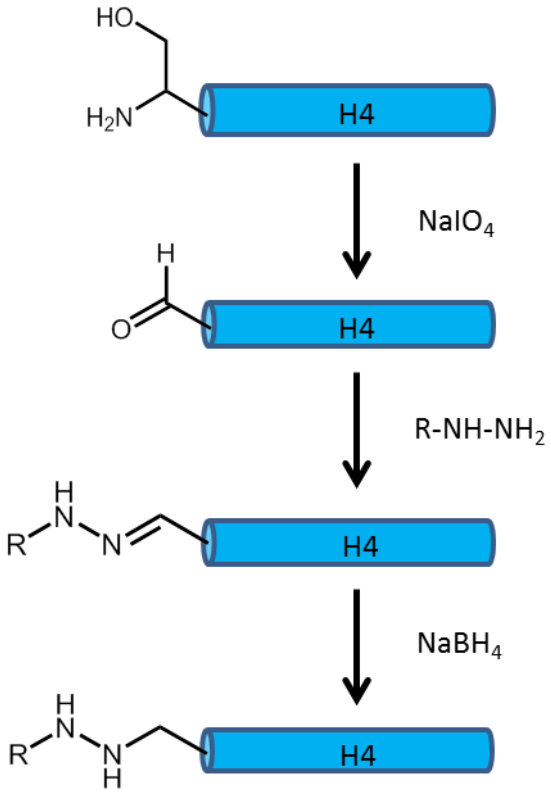

Figure 5. Schematic of N-terminal aldehyde conversion and labeling. R can be any label attached to a hydrazine group, and the hydrazine can be replaced with a hydroxylamine.

Results and Discussion

Aldehyde labeling has been used across a number of biomolecules, but we required an approach that was compatible with histone proteins. We first tested a "one-pot" approach (27), in which all conversion and labeling reagents are added and allowed to react without first removing the

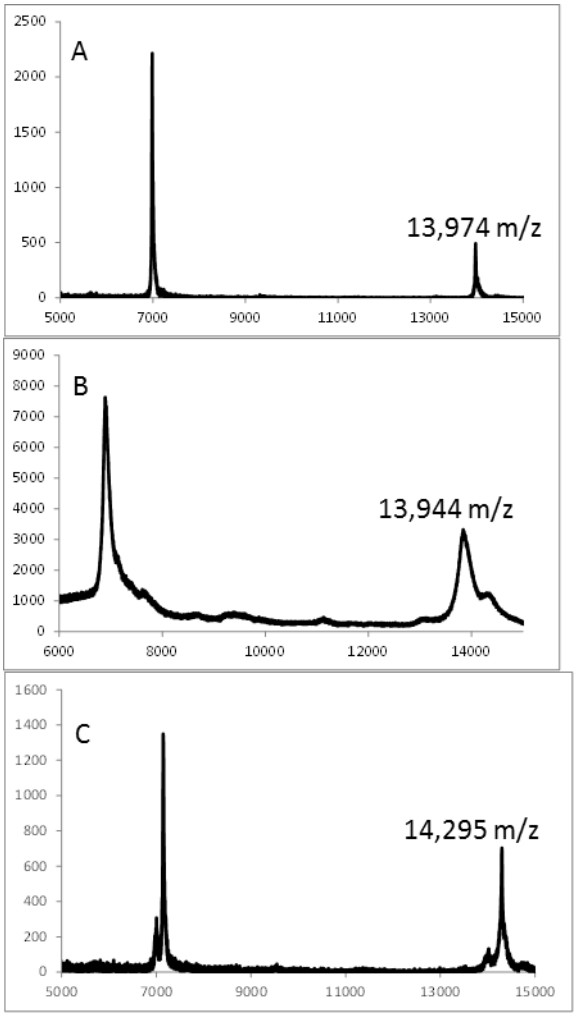

Figure 6. MALDI-TOF analysis of biotin labeling of hH2A. A) 0 hr. hH2A: $[M+H]^+$ observed: *m/z* 13974, expected: *m/z* 13974; B) Aldehyde conversion. Ald-hH2A: $[M+H]^+$ observed: *m/z* 13944, expected: *m/z* 13942; C) Overnight biotin labeling. Biotin-hH2A: $[M+H]^+$ observed: *m/z* 14295, expected: *m/ z* 14297.

oxidizing agent. **Figure 6** illustrates the reaction in which human H2A (hH2A) was treated with sodium periodate and labeled with biotinamidohexanoic acid hydrazide overnight at 4ºC. We found that, for labeling with a biotin hydrazide moiety, the one-pot reaction is sufficient, We also found that a 15-min pause after addition of periodate and before addition of the hydrazide label was required to fully convert the serine into an aldehyde.

The one-pot reaction works efficiently for labeling of proteins and peptides with hydrazide and hydroxylamine compounds (data not shown for tests with *O*-(carboxymethyl)hydroxylamine). However, we found that thiosemicarbazide derivatives, such as the commercially available fluorescein thiosemicarbazide, reacted at multiple sites within the protein when carried out in the presence of unquenched periodate (**Fig. 7**). For these reagents, we developed a stepwise approach. Here, the aldehyde conversion is first performed by treatment with 5mM periodate for 15 minutes, then quenched with glycerol, which contains diols that react with the periodate. Since the glycerol is converted into glyceraldehyde, which would compete with the protein aldehyde for the label, it must be removed by overnight dialysis prior to the labeling. Addition of fluorescein thiosemicarbazide then results in a single label per protein molecule. This is demonstrated with human H2A (hH2A) in **Figure 8**, but is also compatible with histone H4.

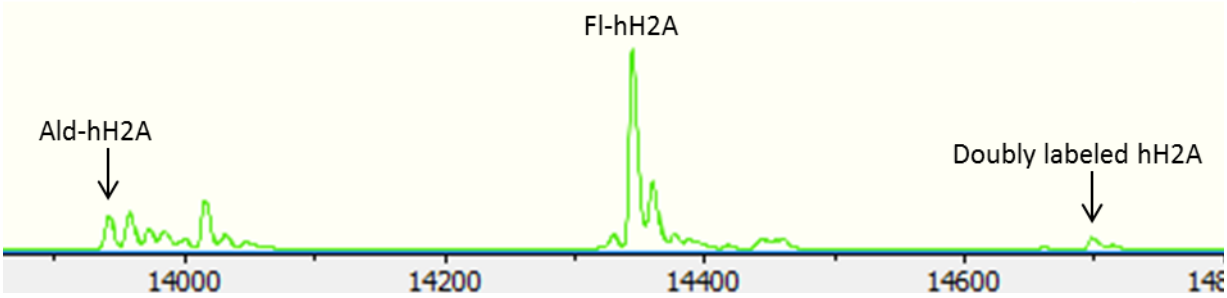

Figure 7. ESI mass spectrometry analysis of one-pot fluorescein labeling of hH2A . Under these conditions, the protein is partially doubly-labeled: ald-hH2A: $[M+H]^+$ observed: *m/z* 13944, expected: *m/z* 13942; fl-hH2A: $[M+H]^+$ observed: *m/z* 14346, expected: *m/z* 14345; doubly labeled hH2A: $[M+H]^+$ observed: *m/z* 14731, expected: *m/z* 14732.

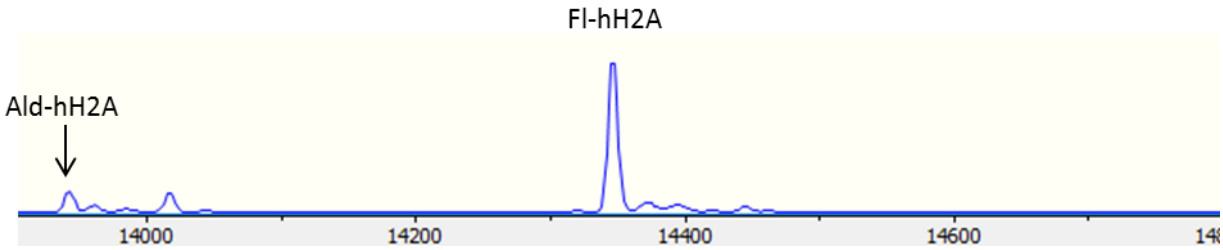

Figure 8. ESI mass spectrometry analysis of step-wise fluorescein labeling of hH2A. The protein is singly labeled with fluorescein. Desired product fl-hH2A: $[M+H]^+$ observed: *m/z* 14349, expected: *m/z* 14346. Unlabeled product ald-hH2A: $[M+H]^+$ observed: *m/z* 13944, expected: *m/z* 13942.

While labeling at an N-terminal aldehyde was successful across multiple reagents tested, we found that the resulting linkage was susceptible to hydrolysis, regenerating free label and aldehyde under the conditions required for our cellular assays for thiosemicarbazide, hydrazide, and hydroxylamine labeling reagents. As a solution, we chose to reduce the double bond by treatment with sodium borohydride to generate a stable linkage. To test the efficiency of the

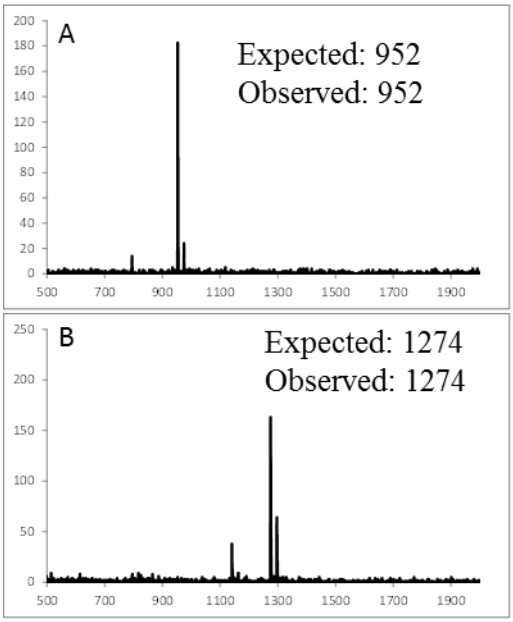

Figure 9. MALDI-TOF analysis of biotin labeling of N-terminal serine peptide. A) unlabeled; B) biotinylated. Expected and observed masses as noted in the figure ($[M+H]^+$). The second highest peak in each spectrum is the sodium salt (+22 *m/z*).

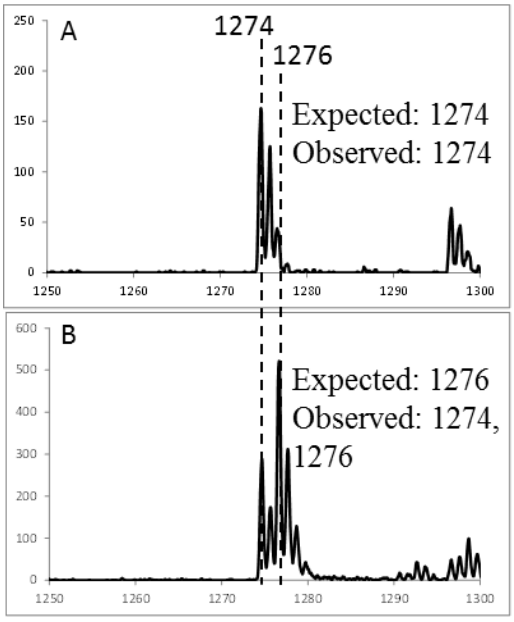

Figure 10. MALDI-TOF analysis of reduction of labeling. A) unreduced; B) reduced. The scale is expanded relative to **Fig. 9** to show fine detail; unlabeled peaks are isotope distribution as expected for natural abundance. Expected and observed masses as noted in the figure ($[M+H]^+$). The peaks near 1300 m/z represent the sodium salt (+22 *m/z*).

reduction, a short sample peptide (SVPFSRV-Dbz, named N-term Ser peptide) with an N-terminal serine was synthesized, aldehyde-converted, biotin-labeled (**Fig. 9**), and reduced (**Fig. 10**). The small molecular weight of the product allowed a resolution of 1 Da in MALDI-TOF MS analysis of the reaction, which was necessary for the evaluation because reduction of a double to single bond adds only 2 Da to the labeled peptide. We found that successful reduction with sodium borohydride first required removal of excess periodate by treatment with glycerol to quench the reagent (data not shown). After periodate removal, the labeled peptide was reduced with 50 mM sodium borohydride at 4 ºC overnight. **Figure 9** shows MALDI-TOF assessment of one-pot biotin labeling of the peptide, illustrating successful aldehyde conversion and labeling. **Figure 10** shows MALDI-TOF MS analysis before and after reduction overnight at 4 °C. Approximately 70% reduction was observed (assuming similar ionization properties). While further optimization would likely increase yields, this is sufficient for our purposes.

In order to simultaneously attach an affinity label and an imaging probe, dual-labeled histones bearing both a biotin and a fluorescein simultaneously were required. To further streamline this process, we used the one-pot approach on a refolded H2A/H2B dimer in which H2A was previously labeled with fluorescein-maleimide at H2A-K119C. Labeling a pre-folded complex would provide an improved workflow, in which readily available Fl-H2A could be refolded with H2B and immediately labeled prior to gel filtration purification, such that both misfolded complexes and excess label would be simultaneously removed. This scheme is depicted in **Figure 11**. Characterization of the labeled product is shown in **Fig. 12**. While MALDI-TOF MS as we carried it out is not fully quantitative, these results suggest that the dimer was predominantly dual-labeled. However, we found that reduction and purification were

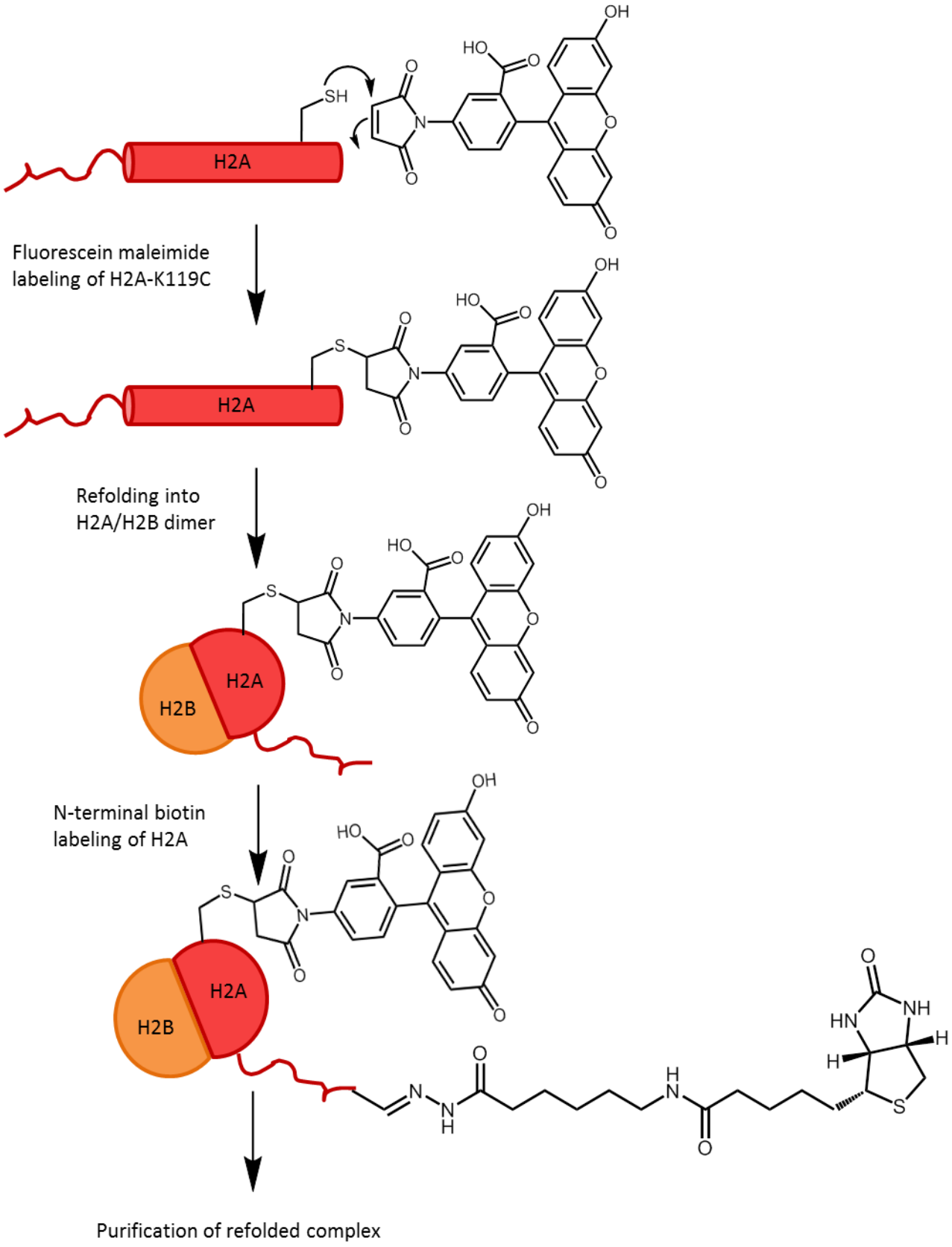

Figure 11. Schematic of double labeling of H2A/H2B histone dimer.

problematic in the context of the folded complex. Borohydride hydrolyzes water, evolving hydrogen gas in sufficient quantities to disrupt complex folding and as well as chromatography. After reduction of a single protein, we typically remove excess borohydride by dialysis (26) prior to refolding, and excess gas does not interfere. While labeling of the refolded complex is efficient and convenient, the best method of label introduction seems to be through labeling of

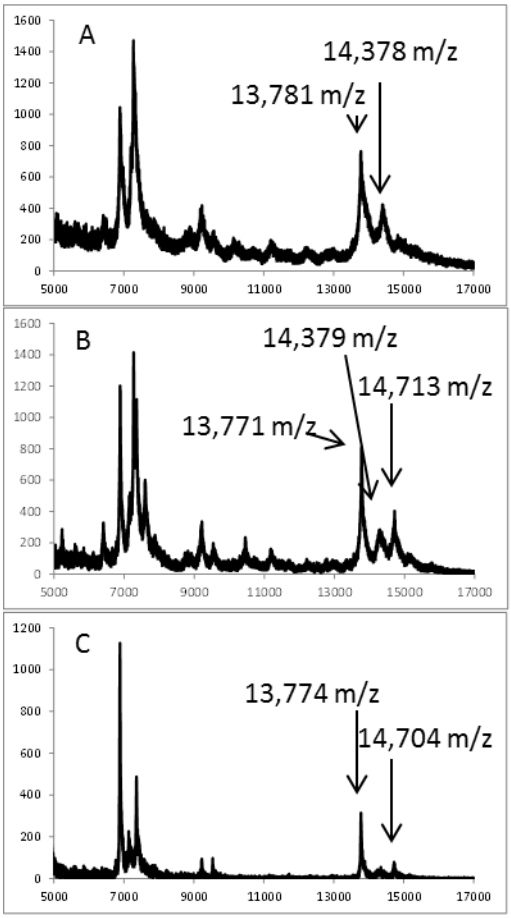

Figure 12. MALDI-TOF analysis of biotin labeling of fl-hH2A/hH2B dimer. **A)** fl-dimer. hH2B: $[M+H]^+$ observed: *m/z* 13781 *m/z* expected: 13772; fl-hH2A $[M+H]^+$ observed: *m/z* 14378, expected: *m/z* 14376; **B)** Biotin labeling of fl-dimer. hH2B: $[M+H]^+$ observed: *m/z* 13771; fl-hH2A: $[M+H]^+$ observed: *m/z* 14379; sodium salt of biotinylated fl-hH2A: $[M+H]^+$ observed: *m/z* 14713, expected: *m/z* 14720; **C)** Biotinylated dimer purified by size exclusion: hH2B: $[M+H]^+$ observed: *m/z* 13774; biotinylated fl-hH2A: $[M+H]^+$ observed: *m/z* 14704, expected: *m/z* 14698.

unfolded, single proteins which can then be refolded into complexes.

Conclusions

We have developed efficient labeling schemes suitable for use with recombinant wild type histones. These approaches can be applied identically to H2A, H4 and semisynthetic and fully-synthetic histones in the future for *in cellulo* study of histone post-translational modifications. We plan to use this technique to introduce fluorescent labels and affinity tags to H4. The fluorescent tags are necessary for cellular imaging, distinguishing between exogenous and endogenous histones in nuclear isolation experiments, as well as quantitation of protein uptake. The affinity tag will be used in pull-down assays to study cross-talk of H4 modifications *in cellulo* via recovery of introduced protein.

Chapter 3: Protein Uptake in *Physarum polycephalum*

Introduction

The myxomycete slime mold *Physarum polycephalum* has been shown to uptake exogenous proteins, particularly histone proteins, through an endocytotic or pinocytotic mechanism. Rather than degrading these proteins, it appears to incorporate them into its cellular machinery (23, 24, 28). *P. polycephalum* has a complex life cycle with multiple different stages mediated by access to nutrients and light. We focus on the plasmodial life stage. In the plasmodial stage, *P. polycephalum* forms large multinucleated cells. In shaken liquid cultures, smaller microplasmodia are the predominant form, but when transferred onto solid medium, the

Figure 13. *Physarum polycephalum* macroplasmodium. Photo Credit: Jerry Kirkhart, under Creative Commons License.

microplasmodia will coalesce into large macroplasmodia that can reach diameters of up to 14 cm (**Fig. 13)** (29). Within the first two cell cycles after coalescence, all the nuclei within one macroplasmodia have synchronous cell cycles (30). Thiriet et al. (2001) has shown not only that *P. polycephalum* uptakes histones into plasmodia but also that these histones are then incorporated into chromatin (31). This property has been used to study the role and importance of histone N-terminal tail regions and nucleosome exchange (24, 31, 32). We hypothesize that synthetic and semi-synthetic histones should be amenable to uptake by *P. polycephalum.* In this chapter, we describe optimization of histone uptake for chemically labeled and for semi-synthetic histone proteins that will enable future study of the role of specific combinations of histone acetylation *in vivo.*

Results and Discussion

Prior to this work, the Ottesen Laboratory had not cultured eukaryotic organisms. The first steps of this work were to develop culturing and handling protocols suitable to carry out uptake experiments. The copious work carried out in this area repeats published protocols, and is therefore not included in this document. Experimental protocols for generation and maintenance of both microplasmodial and macroplasmodial cultures suitable for uptake assays are fully described in Appendix A.

Several parameters must be modulated for successful uptake of histone proteins. First, we find that refolded histone complexes (H2A/H2B dimer, or $H3_2/H4_2$ tetramer) show superior uptake over individual unfolded histones which (data not shown) appear to precipitate nonspecifically in culture media. Second, we find that media must be refreshed, and plasmodia washed, immediately prior to uptake to avoid degradation of protein samples by secreted proteases. Third,

for uptake, concentration of the sample is thought to be key; we maintain at least 1 μM histone as measured on the total complex (not individual histones) for optimal uptake, although some optimization remains to be carried out.

Uptake in Microplasmodia

We first validated uptake of folded histone complexes into *P. polycephalum* microplasmodia, using fluorescently labeled H2A/H2B dimer (fl-H2A-K119C/H2B, labeled using the maleimide method) and labeled $H3_2H4_2$ tetramer (fl-H3-V35C_2/$H4_2$ tetramer, labeled using the maleimide method). Each histone complex was introduced to the external media in microplasmodial cultures for 3 hours at a concentration of 1 μM.

We carried out confocal microscopy of microplasmodia (**Fig. 14**), although imaging protocols were not optimal. After uptake and washing, microplasmodia were visualized using both DIC and fluorescence confocal microscopy. The cells are brightly stained with the fluorophore while

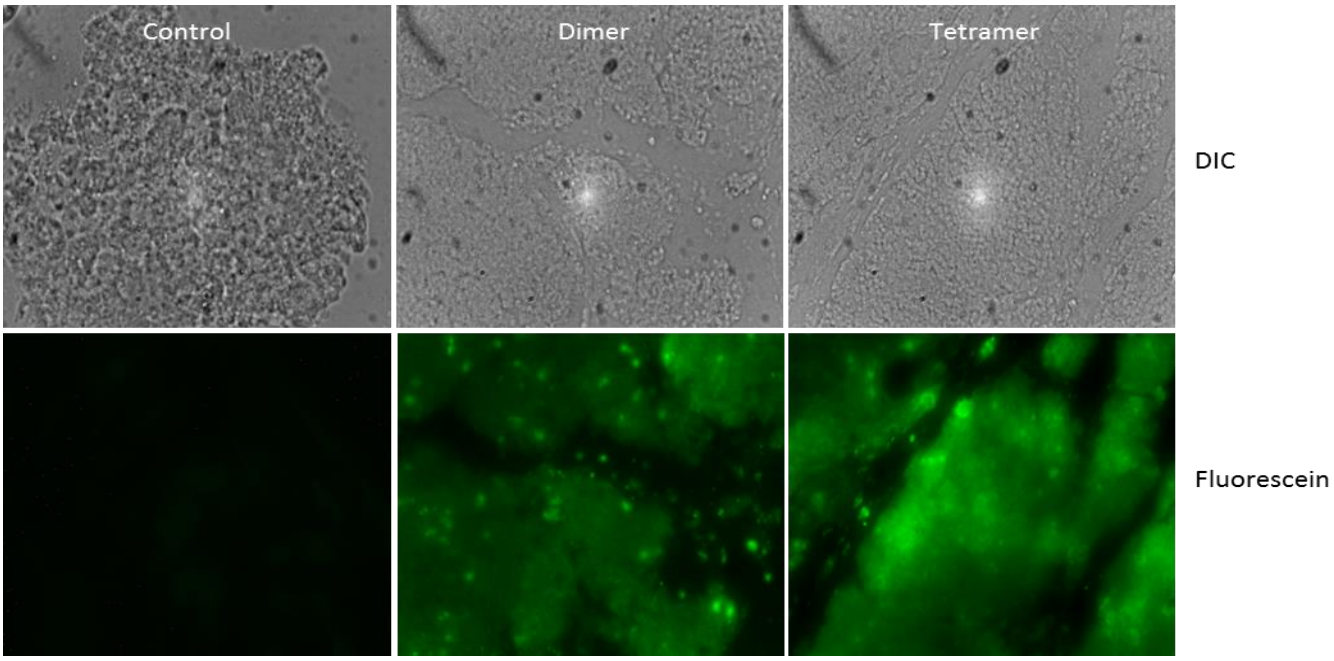

Figure 14. Confocal fluorescent microscopy of uptake in P. polycephalum. 3 hr uptake of fl-dimer and fl-tetramer in P. polycephalum microplasmodia.

the background remains entirely unstained, indicating that the protein entered the cell. As a control, microplasmodia subjected solely to uptake buffer and washing was also imaged, demonstrating that the organism itself does not display significant fluorescence at this wavelength.

To further evaluate the intracellular distribution of exogenous histone, we developed a fractionation protocol to isolate cellular components, especially isolating the nuclei in which we anticipate finding exogenous histone. Cells were harvested after imaging, and then lysed. Nuclei were isolated from lysis pellets using Percoll gradient purification (see Appendix A). Samples were analyzed by SDS-PAGE and visualized by fluorescent imaging via Typhoon scanner (**Figure 15)**. The fluorescence in each fraction was evaluated by analysis with ImageQuant software (data not shown). As expected, significant fluorescence remains in the external media, since uptake is not expected to be complete. For both dimer and tetramer, fluorescence was distributed between the soluble and pellet fractions, suggesting histone is found in both the cytoplasm and the nucleus, although cellular membranes and slime are also found in the pellet

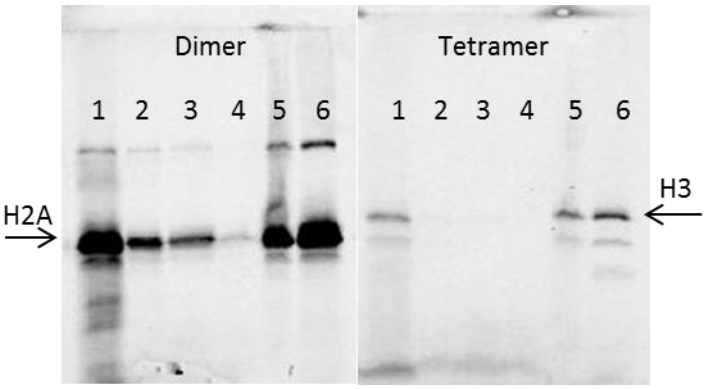

Figure 15. SDS-PAGE analysis of the isolation of nuclei from the experiment shown in Fig. 13. Lanes: 1) external media; 2) soluble fraction; 3) lysis pellet; 4) Percoll sup; 5) isolated nuclei; 6) loading control representing 100% uptake of dimer or tetramer into one fraction.

fractions. Therefore, the pellet was further purified to isolate nuclei, which contained significant fluorescence (Fig. 15, lane 5), which suggests that once the histones enter the cell, they are transported into the nucleus.

Uptake into Macroplasmodia

Microplasmodia can be grown in shaking culture and are convenient to work with, while macroplasmodia grow on a stationary solid surface (filter paper suspended over media). Therefore, microplasmodial cultures are more convenient to work with, but macroplasmodial samples also have some advantages. Since protein uptake is cell cycle dependent (24); one synchronous cell (macroplasmodium) at the right point in its cycle should exhibit higher uptake than many small cells at varying points. We therefore validated uptake of histone dimer (fl-H2A-K119C/H2B) into *P. polycephalum* macroplasmodia.

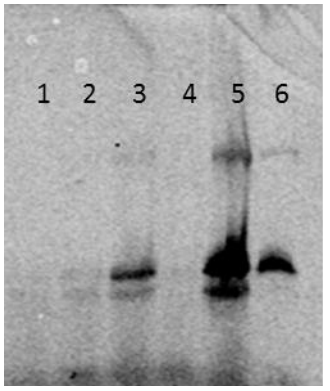

Figure 16. Gel electrophoresis of fl-dimer uptake in macroplasmodia. 3 hour uptake in *P. polycephalum* macroplasmodia. Lanes: 1) external media; 2) soluble fraction; 3) lysis pellet; 4) Percoll sup; 5) isolated nuclei; 6) loading control representing 100% uptake of dimer into one fraction.

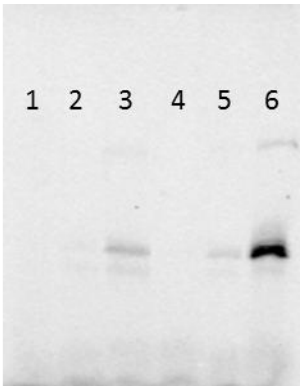

Figure 17. Quantitative loading of **Figure 16.** Lanes 1-6 are the same as in **Figure 16.**

For uptake into macroplasmodia, microplasmodia are allowed to coalesce into one large macroplasmodium which is grown to 2-3 inch diameter. Media is removed from the culture dish, but the surface is not washed. Sample (400 μL of 1 μM complex) is pipetted over as broad as possible an area of the macroplasmodium surface and allowed to absorb for 3 hours. Uptake was assessed by lysis and fractionation (**Fig. 16 and 17**). Uptake did not appear significantly greater than in microplasmodial assays, based on total internal fluorescence. However, histone addition was also not timed to the cell cycle, which takes approximately 9 hours.

In both microplasmodia and macroplasmodia we see some histone uptake, as well as incorporation into nuclei, after 3 h (**Fig. 16**, lanes 3 and 5). In macroplasmodia, some of the exogenous protein appears to be degraded in the media as assessed by the development of a lower band in all lanes. These degradation products then appear to be taken up by the macroplasmodia. This increase in visible degradation might be attributed to the location of our label, which is near the C-terminus of H2A rather than at the N-terminus; fluorescence would therefore be maintained in degradation products. Very little fluorescence is observed in the media/wash after uptake. This is most likely because of higher degradation of that protein rather than higher uptake, since the amount of fluorescence observed in the intracellular components does not add up to the equivalent of full uptake (lane 6 in **Fig 16 and 17**). This would not be surprising, since macroplasmodia typically secrete significant amounts of proteases into the slime layer, which is challenging to remove from the adhered plasmodium. In addition, quantitation is challenging in macroplasmodial cultures, due to the growth form.

Overall, we found that macroplasmodial uptake may provide some benefits, but significantly more histone was required for each macroplasmodial uptake assay, and loading was difficult to control across the uneven cell surface. For the majority of our assays, we chose to continue in

microplasmodia.

Uptake of Semisynthetic Histones

We next sought to carry out the first uptake assay using semi-synthetic proteins. We selected semisynthetic H4 with acetylation at lysine 91 (H4-K91ac). H4-K91ac occurs at the tetramer-dimer interface of the nucleosome core, and is thought to play an important role in chromatin assembly. At the time of this assay, the N-terminal labeling approach had not been fully developed. Therefore, fluorescent tetramer containing H4-K91ac refolded and fluorescein-labeled H3 (introduced as a maleimide at H3V35C) was used for uptake into microplasmodia in shaken culture. Of note, the fluorescein label is not on the semisynthetic histone in this assay; detection is therefore somewhat indirect – while we expect that H3 fluorescence will track with H4 localization, this co-localization has not been directly demonstrated.

After 3 hr of uptake, cells were harvested, nuclei were isolated, and all cellular fractions were analyzed by SDS-PAGE with fluorescent imaging to track histone H3 (**Fig. 18**). Fluorescence is

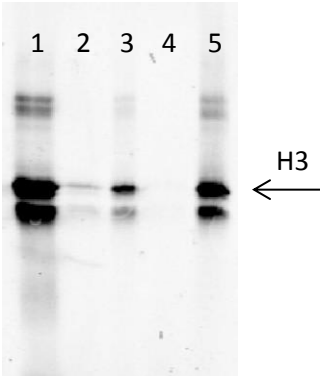

Figure 18. Uptake of H4-K91ac fl-tetramer into *P. polycephalum*. Lanes: 1) external media; 2) soluble fraction; 3) lysis pellet; 4) Percoll sup; 5) isolated nuclei.

observed in the soluble fraction (cytoplasm) and in isolated nuclei. Localization into the nucleus strongly suggests that these histones were also incorporated into chromatin, although isolated mononucleosomes were not directly observed. Taken together, this suggests the first uptake of a semisynthetic histone with a biologically relevant post-translational modification into a eukaryotic cell.

Development of pull-down assays for exogenous histones introduced to *P. polycephalum*

While fluorescent labels are sufficient to visualize the exogenous histones after uptake, downstream direct analysis of the incorporated histone requires a mechanism to recover the protein from the cellular context. We develop this with a dual labeling approach in which both fluorescein and biotin were simultaneously introduced to folded histone dimer, which allows avidin capture of the introduced dimer. To do this, we labeled H2A with fluorescein maleimide as described in Chapter 2. This fluorescent protein was refolded into H2A/H2B dimer, which was then labeled a second time with a biotin tag at the N-terminus of H2A using aldehyde conversion **(**see **Fig. 11)**. Histones are notoriously susceptible to avidin pull-down if rigorous

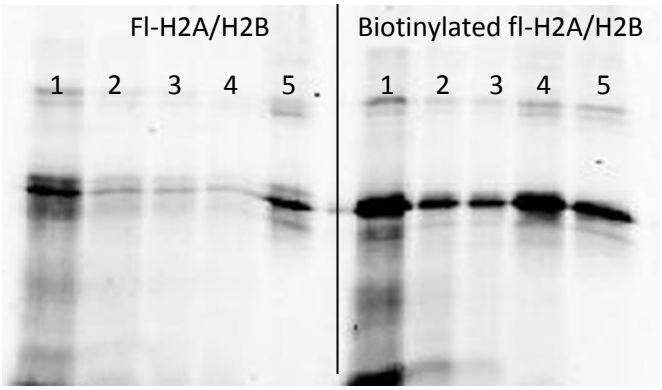

Figure 19. Uptake of fl-H2A/H2B (left) and biotinylated fl-H2A/H2B (right). SDS-PAGE analysis of nuclear isolation. Lanes: 1) external media; 2) wash 1; 3) wash 2; 4) soluble fraction; 5) purified nuclei.

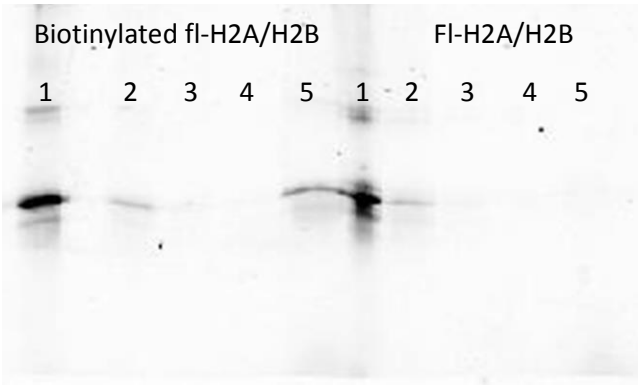

Figure 20. Avidin pull-down from isolated nuclei**.** Lanes: 1) input; 2-4) washes 1-3; 5) elution from beads. Left: biotinylated fl-H2A/H2B, right: fl-H2A/H2B

care is not taken to minimize interactions (33). Therefore, significant optimization was carried out prior to this uptake assay.

The folded, dual-labeled dimer was introduced to *P. polycephalum* microplasmodia for 3 hours of uptake. As a pull-down control, fluorescein-5-maleimide-labeled dimer lacking the biotin affinity tag was introduced to a second culture. After 3 hours of uptake, cells were harvested and nuclei were isolated and assessed by SDS-PAGE. **Figure 19** illustrates that both fl-H2A/H2B (left) and biotinylated fl-H2A/H2B (right), were taken up by the microplasmodia and transported into the nuclei.

The nuclei were lysed by sonication and treated with MNase to digest chromatin into individual mononucleosomes. Histones were pulled down onto magnetic beads coated with monomeric avidin in the presence of 20% glycerol and washed extensively. Beads were analyzed by SDS-PAGE with fluorescent imaging (**Fig. 20).** Fl-biotin-H2A is observed on beads, but Fl-H2A in the absence of biotin was not (**Fig. 20**, each lane 5). This demonstrates successful pull-down of exogenous biotin-labeled histone as well as a lack of non-specific binding of Fl-H2A. These pull-down assays will be further developed for total analysis of recovered mononucleosomes, as

well as further analysis of the retained biotinylated exogenous histone by mass spectrometry.

Conclusions

In this chapter, we demonstrate successful uptake of chemically labeled histones into *P. polycephalum* microplasmodia and macroplasmodia. These histones appear to be transported into nuclei, suggesting that they are deposited into chromatin. Together with the first successful introduction of an exogenous semisynthetic histone directly into a eukaryotic cell, these findings support *P. polycephalum* as a good system for *in vivo* study of synthetic modified histones to elucidate the functions of and cross-talk between histone modifications.

Chapter 4: Histone Uptake in Other Cell Lines

Introduction

There is some discrepancy in the literature as to whether histone uptake is a unique property of *P. polycephalum*. The highly positively charged, unstructured tails of histone proteins share some properties with cell-penetrating peptides. Taken together with an opportune culture error in which we observed histone uptake into a contaminant organism, these suggested that histone proteins might have cell penetrating properties that would allow uptake in higher order eukaryotic cells. Here, we explore histone uptake in a variety of eukaryotic cells, culminating in successful uptake into mammalian and human cells.

Results and Discussion

Mucor

By culture error, a contaminant organism was introduced to the *P. polycephalum* cultures early on in the project. Because it was introduced so early, and since the laboratory had no experience with the expected growth pattern and appearance of the slime mold, this error remained undetected for some time. As a result, histone uptake experiments were conducted on this organism. Interestingly, successful uptake was observed.

In these assays, fluorescently-labeled histone dimer (fl-H2A-K119C/H2B, maleimide-labeled) was added to a shaken culture. After 1 hour of uptake, fluorescence was observed in the soluble fraction of the cell and in some component of the lysis pellet (**Fig. 21**).

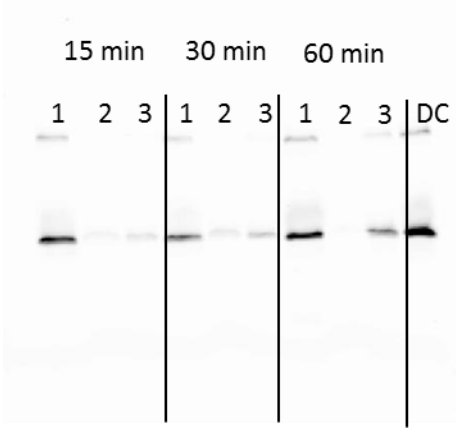

Figure 21. Uptake of fl-dimer in Mucor. Time course of uptake into soluble and insoluble fractions over 1 h. 1) media; 2) soluble fraction; 3) lysis pellet; DC) loading control representing 100% uptake into a single fraction.

We immediately set out to identify the contaminant organism. Primers were designed to amplify the 18s ribosomal DNA. Because ribosomal DNA is relatively conserved between species, this technique allows primers that anneal to highly conserved regions to be used. At the same time, enough variations exist between ribosomes that the alignment results can provide information about the originating organism. Sequencing results are provided in **Fig. 22**, and alignment using BLAST, allowed the identity of the contaminant to be narrowed down to the Mucor genus, a collection of mold species that are common to the Ohio area. (34, 35). Mucor is a true mold that resides in soil, digestive systems, and plant material. It is a common laboratory mold and contaminant. Certain species of Mucor have been studied in depth as both pathogens and biofuel producers (35, 36).Slime molds, despite the name, are not fungal organisms but rather amoebal species. True molds have many different qualities such as cell walls that would complicate protein uptake. No existing evidence suggests that any mold can uptake protein the way that *P*.

NNNNNNNNNNNNNNNGCANNTNCGAAGATNTTCNNGCNNNNNAGGNCN
GNNNNNGANNANNTACANTGNTGNATNNNNNNNNNGNCTNGTATGGGGGT
GAGGACGGNGTAGCTCGNNNAACGACGATCCGTGGNCGTGNNNATCCGGT
GCTCTTTTGNGTGGATGCTTANGGTCCATACTTTGGCCATATCAAAGNTAGC
GATTTGCNNGGTTAATTNANTTTTAGTCTTTAGATGAGGTGGCCTGGTCTTC
NTTGATCAAGCTCGCTTTTATCGANACTTTTTTTCTGGTTATGCTATGAATA
GCTTCGGTTGTTTANAGTCNCTAGCCAGATGATTACCATGAGCAAATNAGA
GTGTTTAAAGCAGGCTTTCAAGCTTGAATGTGTTAGCATGGAATAATGAAA
TATGACTTTAGTCCCTATTTCGTTGGTTCAGGAACTTAAGTAATGATGAATA
GAAACGGTTGGGGACATTTGTATTTGGTCGCTAGAGGTGAAATTCTTGGAT
TGACCGAAGACAAACTACTGCGAAAGCATTTGATCCAGGACGTTTTCATTG
ATCAAGGTCTAAAGTTAAGGGATCGAAGACGATTAGATACCGTCGTAGTCT
TAACCACAAACTATGCCGACTAGAGATTGGGCTTGTTTATTATGACTAGCTC
AGCATCTTAGCGAAAGTAAAGTTTTTGGGTTCTGGGGGGAGTATGGGACGC
AAGGCTGAAACTTAAAGGAATTGACGGAAGGGCACCACCAGGAGTGGAGC
CTGCGGCTTAATTTGACTCAACACGGGGAAACTCACCNNTCCAGACATAGT
AAGGATTGACAGATTGAAAGCTCTTTCTAGATTCTATGGGTGGTGGTGCAT

Figure 21. Sequencing results from PCR of 18s DNA.

polycephalum does. Regardless, histones appear to penetrate cells of the Mucor genus, a category of true molds.

As a potential negative control, GFP (1 μM) was introduced to the true mold for 1 hr and analyzed by confocal fluorescent microscopy (**Fig. 23**). In the image, the edges of cells are lightly stained, but none of the fluorescence from GFP is found inside the cell. This implies that the protein is binding to the outside of the cells but not crossing the membrane, as would be expected for most proteins. This evidence supports the suggestion that import of histones into this organism is a unique property of histone proteins. We hypothesized that these proteins could also penetrate higher eukaryotic cells, possibly mediated by the unstructured, positively charged tails that resemble cell-penetrating peptides (CPPs).

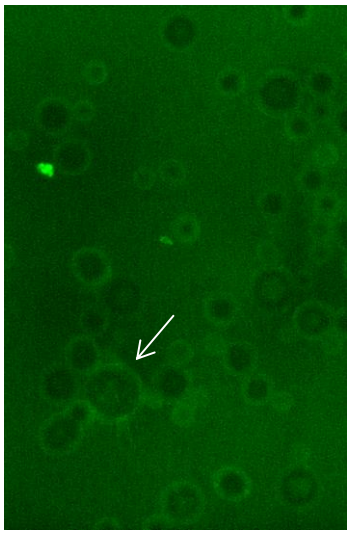

Figure 23. GFP in Mucor. Fluorescent microscopy of cells after GFP uptake and washing. Note that the majority of the above-background fluorescence occurs at the perimeters of cells (arrow).

Rat Intestinal Endothelial Cells

We hypothesized that exogenous histones would successfully enter the cells of a higher eukaryote by exploiting the CPP-like properties of the histone tails. To test this, cultured rat

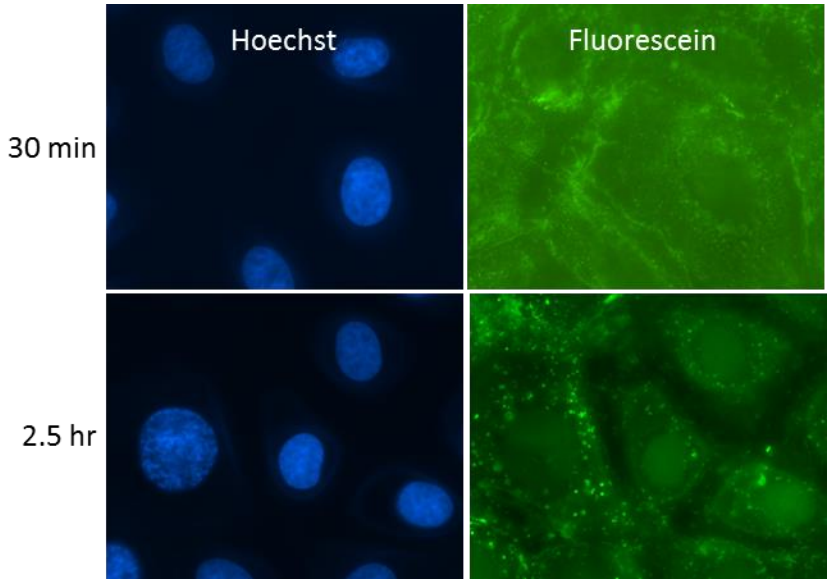

Figure 24. Live fluorescence microscopy of Fl-H2A/H2B uptake in rat IEC cells: Left: Imaging on Hoechst. Right: Imaging on fluorescein.

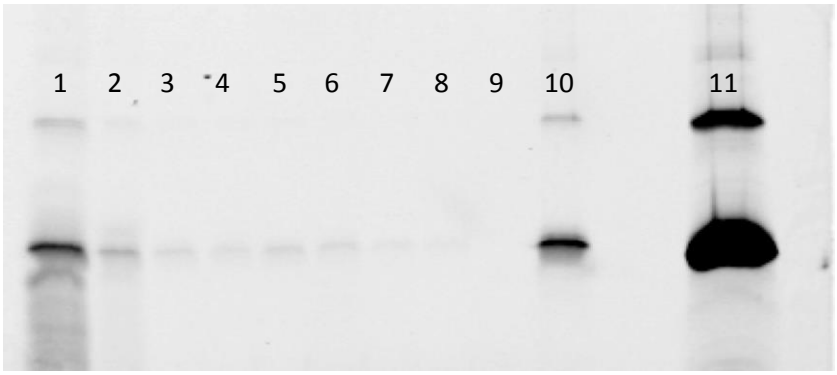

Figure 25. Uptake of fl-dimer in adherent rat intestinal endothelial cells. Lanes: 1) external media; 2-5) PBS washes; 6-8) supernatants from three consecutive lysis steps; 9) Percoll gradient supernatant; 10) isolated nuclei; 11) dimer control representing 200% uptake into a single fraction.

intestinal endothelial cells were acquired from Dr. Elena Kudryashova (OSU). Fl-H2A-K119C/H2B (1 μM) was added to adherant IEC2 cells, and uptake was followed by live cell fluorescent microscopy for 3 hours (**Fig. 24**). After 2.5 hours, fluorescence appeared to cluster co-localized with Hoechst stain, which suggested but did not demonstrate nuclear accumulation of fluorescent histone.

After 3 hours, cells were harvested and nuclei were isolated. All cellular fractions were analyzed by SDS-PAGE and analyzed by fluorescent imaging (**Fig. 25**). The majority of the exogenous histones were split between the external media (lane 1) and the nuclei (lane 10), suggesting efficient transport and accumulation of the histones in the nuclei after uptake. Interestingly, while degradation bands are visible in the media, there appears to be little intracellular degradation.

Live cell microscopy in HeLa cells

Live cell fluorescence imaging was also used to visualize uptake of fluorescein-maleimide-labeled dimer into cultured HeLa cells (also provided by Dr. Elena Kudryashova) (**Fig. 26**). First,

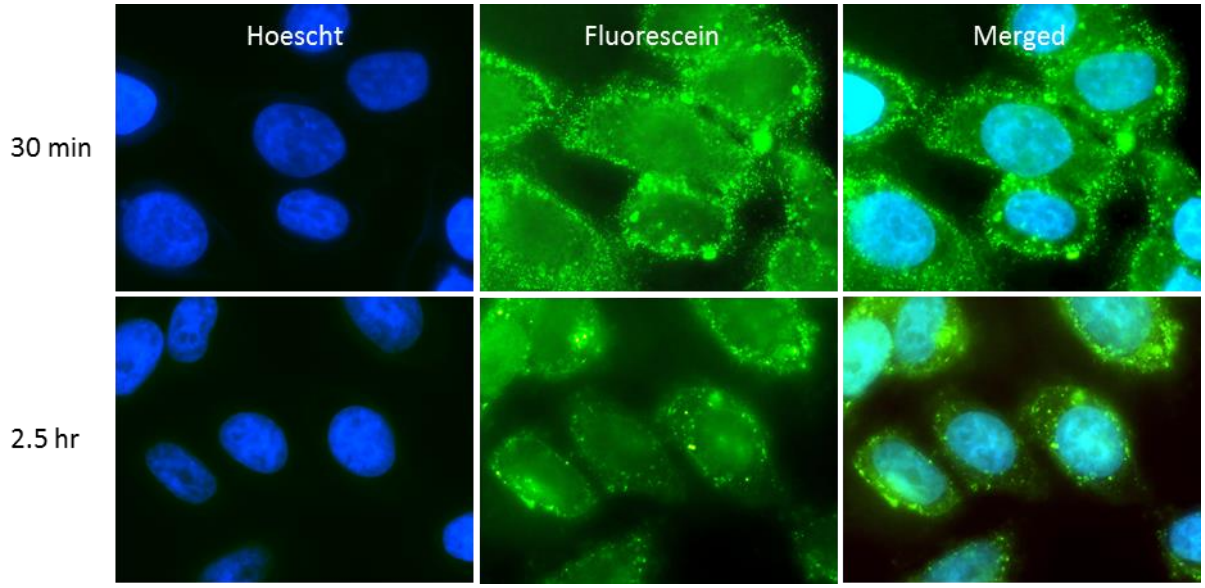

Figure 26. Live fluorescence microscopy of Fl-H2A/H2B uptake in HeLa cells: Left: Imaging on Hoechst. Middle: Imaging on fluorescein. Right: Merged fluorescence.

labeled dimer was introduced to the surface of the adherent cells for 30 min, and the cells were thoroughly washed and imaged. Fluorescence was present in the cells while the background was dark, showing efficient uptake in only half an hour. Hoechst staining of nuclei shows colocalization of some of the fluorescein with chromatin. Punctate staining was highly evident, most likely representing fluorescent dimer encapsulated within endosomes. After washing, cells were followed for 2.5 h without further addition of histone. Continued colocalization of some fluorescence with Hoechst stain for chromatin, mildly increased over background, suggests additional accumulation of histones in the nucleus over this time. In addition, reduction in the punctate staining suggests that dimer is either degraded in endosomes, or escapes to reach the cytoplasm and the nucleus. This analysis is somewhat limited by the live cell microscopy because of its inability to distinguish between exogenous histones on the surface of nuclei and histones that have been transported into the organelle, as well as photobleaching of the fluorescein fluorophore with repeated imaging. Confocal microscopy is required to truly

demonstrate transport of histone proteins into the nucleus, which we demonstrate in MDA-231 cells.

MDA-231 Cells

Human breast cancer MDA-231 cells were acquired (Dr. Michael Freitas, OSU Medical Center). Fl-H2A-K119C/H2B (maleimide-labeled) was added at a concentration of 1 μM and uptake was allowed to proceed for 1 hour. Cells were thoroughly washed, fixed, and treated with Hoechst stain for comparison to chromatin. Confocal microscopy was performed (CMIF), and cells were imaged on DIC, Hoechst, and fluorescein (**Fig. 27**).

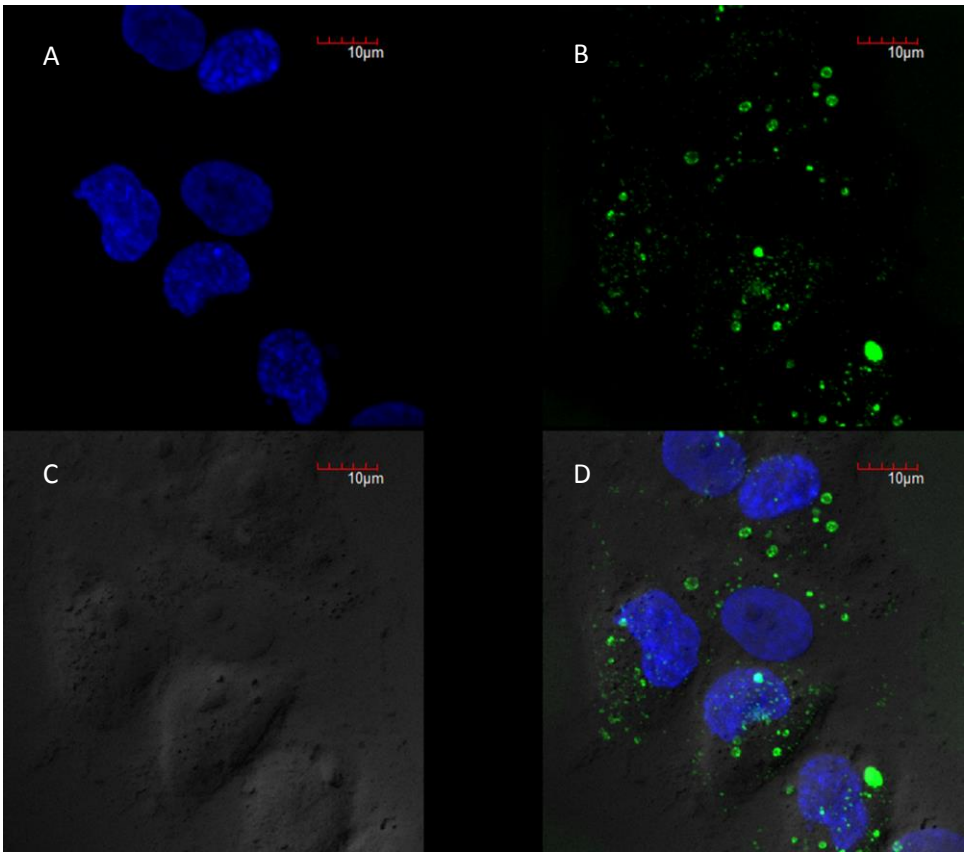

Figure 27. Confocal microscopy of fl-dimer uptake in human breast cancer MDA-231 cells. A) imaging on Hoechst; B) imaging on fluorescein; C) phase contrast; D) merged view.

Fluorescein (green) is clearly visible within the cell after one hour of uptake. Further, there is clearly at least some colocalization of chromatin (Hoechst stain, blue) and fl-H2A (green), which demonstrates that histones are entering the nucleus, although perhaps not at high amounts.

A clearer picture of the colocalization was obtained through a 3D reconstruction of each confocal

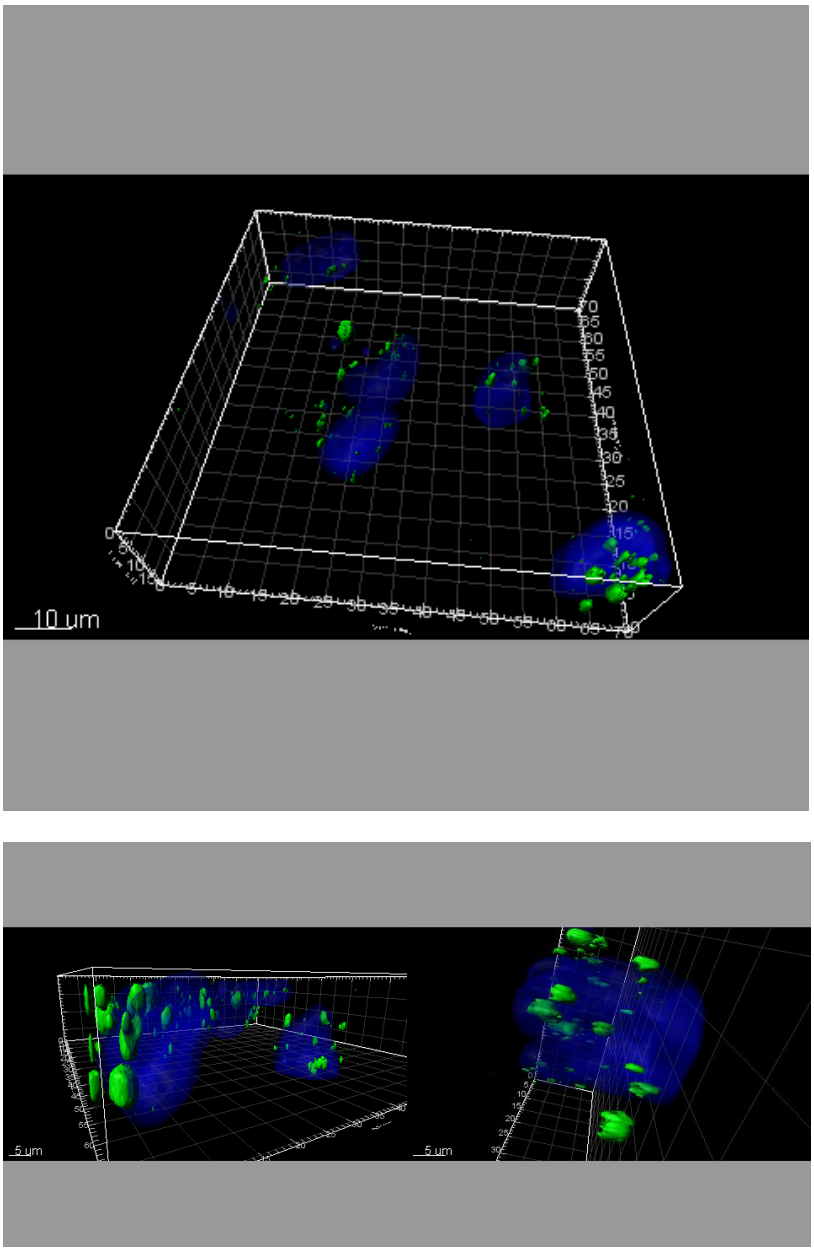

Figure 28. 3D reconstruction of fl-dimer in human MDA-231 cells. Three different views of a 3D reconstruction of each layer of confocal microscopy.

layer. **Figure 28** shows the same 3D reconstruction from three different angles. While some of the exogenous histone has entered nuclei after one hour of uptake, the majority remains in focused clusters, concentrated near the nuclear membrane and often in clefts pushed up against the nucleus. This suggests that dimer may localize to the golgi or the endoplasmic reticulum before being transported into the nucleus.

Of note, these images were acquired after one hour of uptake, which is significantly shorter than the typical uptake assay carried out. It would therefore not be unexpected for the histones to accumulate in an intermediate stage of transport. Future plans include time course experiments to determine optimal uptake times, and to observe the transport pathway in these human cells. However, it is highly encouraging to see clear accumulation of histones in the nucleus, even at these early stages of uptake.

Conclusions

Our preliminary data suggests that histones are taken up by several different types of eukaryotic cells, and supports the hypothesis that the positively charged, unstructured histone tails act as cell penetrating peptides. This hypothesis spurred uptake experiments in rat IEC and human cancer cells. Analysis of histone uptake and incorporation into these cell lines shows not only cellular uptake but nuclear localization of the exogenous histones. Taken together, this implies that histone proteins display inherent cell-penetrating characteristics.

While protein uptake and incorporation has been closely studied in *P. polycephalum*, a few studies have demonstrated histone uptake in higher cell lines as well. According to the literature, histone proteins penetrate the cell membranes of both plant protoplasts (37) and of human cancer cells (38, 39), and that this uptake might be partially endocytosis-independent under the

conditions used. However, these studies were also carried out using unfolded histone proteins which, in our hands, precipitate under the uptake conditions reported. It has also been suggested that covalent linkage of H2A to bovine serum albumin increased protein uptake (37-39).

Taken together with our studies, these results suggest that histone proteins display cell penetrating characteristics, a property that would allow study of synthetic histones in mammalian or human cell lines. These systems provide studies with greater relevance, especially given the connection of histones and their modifications with cancer and other genetic diseases.

Chapter 5: Conclusions and Future Directions

The goal of this project was to establish a means of easily introducing exogenous, chemically modified histone proteins into a eukaryotic cell. This uptake will permit study of chemically-modified histones to move from *in vitro* analysis to *in vivo* experimentation. Interactions between the cell's complex environment and the exogenous modified proteins can then provide a greater and more nuanced understanding of the functions of and crosstalk between histone PTMs.

Successful incorporation of exogenous histones has been demonstrated in *P. polycephalum* microplasmodia and macroplasmodia, including the first demonstration of direct uptake of a semi-synthetic PTM-bearing histone protein by a eukaryotic cell. Not only do we observe uptake into whole cells but also incorporation into nuclei. We plan to conduct time courses of uptake in microplasmodia to determine the time at which the highest amount of exogenous histones are incorporated into the cell and into nuclei. A similar time course will be conducted in macroplasmodia with synchronous nuclei and monitoring of the cell cycle. This will be performed first to determine if histone uptake is cell cycle dependent and second to analyze possible advantages of uptake of histones into macroplasmodia at the correct point in the cell cycle over uptake into non-synchronous microplasmodia. We also aim to isolate mononucleosomes containing exogenous histones to directly demonstrate that histone proteins are not only transported into the nucleus of *P. polycephlum* but also deposited in chromatin.

In addition to successful incorporation of exogenous histones into *P. polycephalum*, uptake was observed in higher order eukaryotic cell cultures. Incorporation of exogenous histones into fungal, mammalian, and human cells and nuclei suggests that histones display cell penetrating characteristics. This allows study of semi-synthetic and synthetic histone proteins with defined

sets of histone PTMs not only in an amoebal slime mold but also in mammalian and human cells, increasing the relevance of the discoveries made about the functions of these modifications. A time course of histone uptake in human cells is planned to study the temporal parameters of uptake of exogenous histones into cells and subsequent transport into nuclei. Confocal microscopy will be used to monitor this process to obtain the most accurate depiction of the process. Biotin pull-down techniques will also be developed for this system so that the introduced proteins can be recovered from the cellular environment.

Our immediate plans are to use these combined techniques to determine the effect of H4-K91ac on intracellular histone transport, on chromatin deposition rate, and in modification crosstalk. This modification is located at the tetramer-dimer interface and has been shown to destabilize the nucleosome. Interestingly, it has also been found to be associated with the Hat1p-Hat2p-Hif1p chromatin deposition complex, indicating that it may be necessary for the incorporation of H4 into the nucleosome, and has been implicated in acetylation of H4 at K5 and K12 (7). We will study this connection *in vivo* by comparing chromatin deposition of wild type H4 to that of the modified protein, produced by partial chemical synthesis of the protein. This will also be compared to chromatin deposition of H4-K91Q, where the lysine has been replaced by the acetyllysine mimic glutamine. Other unpublished work in the laboratory has suggested that nucleosomes reconstituted with H4-K91Q have an intermediate stability between unmodified and H4-K91ac nucleosomes, but in a cellular context the most important difference might be that while H4-K91ac can be deacetylated and is thus a dynamic modification, H4-K91Q is static. Since chromatin maturation is associated with loss of H4-K91 acetylation, this difference may be important.

Secondly, we will look at the crosstalk between H4-K91ac and other modifications both on H4 and throughout the nucleosome. Using the labeling technique discussed in Chapter 2, we can attach a biotin pull-down tag to the N-terminus of H4, allowing us to introduce the protein to a cell and then pull it back out. We can then analyze the protein to determine the modification state, or analyze a complex to determine binding partners. Since we can fractionate cytoplasmic fraction, nuclear fraction, and chromatin, this will allow us to characterize the binding partners and current modifications in a variety of contexts. These studies will be analyzed by mass spectrometry in collaboration with Dr. Michael Freitas to obtain a highly accurate characterization of the isolated molecules. Interestingly, we have found in preliminary studies that we can pull down entire mononucleosomes using a biotin-tagged histone, and then eliminate all but the tagged histone with high-salt washes, which will allow us for the first time to determine the dependence of the precise modification status of noncovalently linked histone proteins within a mononucleosome on the modification state of the probe protein. This study will elucidate the way a cell responds to a histone with a specific set of modifications by changing that modification set and potentially reveal new functional relationships between histone modifications, and possibly of the so-called histone code. These studies open up entirely new directions in the study of epigenetic histone modifications in the context of the human cell.

Appendix A: Methods

Cell Culture and Handling

Generation and Handling of *Physarum polycephalum* Cultures

SDM (semi-defined media): 17 mM citric acid, 0.3 mM $FeSO_4$, 1.5 mM KH_2PO_4, 2.4 mM $MgSO_4$, 0.4 mM $MnCl_2$, 0.1 mM $ZnSO_4$, 4 mM $CaCl_2$, 10 mg/mL tryptone, 10 mg/mL glucose, 1.5 mg/mL yeast extract, corrected to pH 4.6 with 6M HCl

Hemin stock: 0.05% (w/v) hemin chloride in 1% NaOH

All growth methods should be carried out using strict aseptic technique to prevent contamination with bacteria or mold strains. All pipette tips, beads, and filter paper should be autoclaved regularly. Fresh gloves should be worn, the benchtop and pipettes should be ethanol-sterilized, and a lit Bunsen burner should be nearby whenever cultures are handled.

To start a plate from dried sclerotia, one piece of filter paper containing *Physarum polycephalum* (m3c) sclerotia is deposited face down on another filter paper suspended on glass beads in a petri dish. The bottom of the dish is filled with 12 mL of medium (1 mL of 0.05% hemin stock/100 mL SDM). Plate cultures are incubated at room temperature (~22-25 °C) in a dark environment to prevent sporulation, refreshing the media periodically to allow continued growth. These cultures take between 3 and 7 days to cover the plate (24).

When the culture has spread to cover the majority of the plate, it should be split to inoculate a new plate. To do this, a petri dish is prepared with beads, filter paper, and media. A scraping of the older culture is then transferred to the new plate with an ethanol-sterilized microspatula. A

plate culture can be grown from an inoculate from a liquid culture, but it requires a longer period of time before it begins to grow across the plate (24).

For a liquid culture, 50 mL of media are inoculated with either a small scraping from a plate culture or 0.5 mL of a fully-grown liquid culture. Liquid cultures are incubated at 25 °C with shaking at 180 rpm. These cultures should be autoclaved twice before inoculation; once before addition of media and once after. A liquid culture takes between 3 and 7 days to reach workable density. A healthy liquid culture is identified by a high density of large, yellow microplasmodia surrounded by clear media. The presence of cloudy media and small microplasmodia indicates that the cell density is too high (24).

Uptake in *P. polycephalum* microplasmodia and Mucor

Microplasmodia from liquid culture were washed twice in fresh media to remove external, excreted proteases and resuspended in fresh media. Cells were centrifuged at 50*g*. Higher speeds may lead to premature cell lysis. Protein was added to 1 µM, and the cells were incubated for 3 hours at 25°C with shaking in the dark. Cells were then washed twice in wash buffer (20 mM Tris pH 7.5, 1 mM EDTA), resuspended in isolation buffer (15 mM Tris pH 8, 15 mM $MgCl_2$, 5 mM EDTA, 1 mM PMSF, 0.25 M hexylene glycol, 0.6% Triton X-100, 3 mM DTT), and sonicated for ten 1-second pulses at 70% amplitude. Cells were then spun at 1,200*g* for 5 minutes to separate the soluble fraction. Uptake and analysis of Mucor cells followed this same technique.

The pellet was then resuspended in 10 pellet volumes of 25% Percoll in isolation buffer and spun at 52,500*g* for 20 minutes. The nuclei formed a visible ring near the bottom of the gradient. Isolated nuclei were washed three times in MNase digestion buffer (10 mM Tris pH 8.0, 60 mM

KCl, 15 mM NaCl, 1 mM $CaCl_2$), and 1 U/µL MNase was added. Samples were heated to 37°C for 5 minutes, and the MNase was quenched with 10 mM EDTA (40). Digested nuclei were then sonicated gently (5 x 1 sec, 70% amplitude) to break nuclei, freeing nucleosomes into the soluble portion after centrifugation at 1500*g* for 5 min.

Uptake in *P. polycephalum* macroplasmodia

Macroplasmodia can be generated from shaken cultures of microplasmodia. To do so, 50 mL of microplasmodia were centrifuged at 50*g* for 5 min, and the media was removed. The cells were washed with 10 mL of sterile water, resuspended in 1 mL of sterile water, and deposited on filter paper suspended on glass beads in media in a petri dish. The high density of the cells causes them to coalesce into a macroplasmodium. The macroplasmodium was allowed to grow to a diameter of 2-3 inches before uptake (24).

Media was removed from the bottom of the dish prior to addition of exogenous protein. The protein solution (400 µL, 1 µM) was spread over as much of the surface of the macroplasmodium as possible. After the uptake time, the cell was soaked twice in 1 mM EDTA for 10 min each. It was then scraped off the filter paper and resuspended in isolation buffer. The mixture was homogenized to lyse the cell (10 gentle strokes) and then centrifuged at 1200*g* for 5 min. Further lysate treatment is the same as with microplasmodia (24).

Culture and Uptake in Mammalian Cells

Rat IEC and HeLa cells were generously donated by the Kudryashov laboratory, and microscopy of these cells was performed using their live cell fluorescent microscope. Human MDA-231 cells were donated by the Freitas laboratory. Before addition of exogenous protein, cells were washed twice with PBS. Uptake in mammalian cells was performed identically to that in *P.*

polycephalum and Mucor for the time specified in the results. After uptake, cells were washed at least three times with phosphate buffered saline and centrifuged at 1000*g* for 10 min. The adherent cells were then trypsinized with TrypLE™ (Life Technologies) to remove them from the growth surface and then lysed with NP-40 buffer (10 mM Tris pH 7.5, 5 mM $MgCl_2$, 10 mM NaCl, 0.5% NP-40). The lysis mixture was incubated on ice for 5 min then centrifuged at 500*g* for 5 min. Lysis was repeated 3x. Purification of nuclei followed the same protocol as isolation of nuclei from *P. polycephalum* (41).

Microscopy

To fix cells, they were first washed twice with wash buffer (20 mM Tris pH 7.5, 1 mM EDTA). Formaldehyde was added to the resuspended cells to 4% final concentration and incubated on ice for 15 min. The cells were then pelleted (50*g*, 5 min) and washed with wash buffer. To stain nuclei with Hoechst, the dye was added to the resuspended cells to 1 µg/mL final concentration and incubated on ice for 15 min. The cells were washed once more with wash buffer and plated on microscopy slides. Microscopy of *P. polycephalum* was performed using the confocal fluorescent microscope from the Hopper laboratory. Human MDA-231 microscopy was performed by the Campus Microscopy and Imaging Facility (CMIF).

Biotin Pull-down

Glycerol was added to digested nuclei to 20%. The mixture was then combined with magnetic monomeric avidin beads that had been washed with MNase digestion buffer. Proteins were allowed to bind for 10 minutes on ice. Beads were then washed (3 x 100 µL) in MNase digestion buffer + 10% glycerol (42). A small sample of beads was then run on a gel to ensure pull down. To elute from beads for SDS-PAGE analysis, a small sample of beads were boiled in SDS

loading dye for 5 min. Beads were pelleted before loading. To elute from the beads for mass spectrometry purposes, the beads were soaked in 5% formic acid for 15 minutes on ice. These samples were then lyophilized to dryness.

PCR of rDNA

Cells of the unknown organism in liquid culture were lysed by heating at 100ºC in the presence of 5 mM phenylmethylsulfonylfluoride (PMSF) for 5 min. The lysate was then centrifuged at 3000*g* for 10 min. The supernatant was then used as the template in a polymerase chain reaction using a forward primer with the sequence 5`-CCGGAGAAGGAGCCTGAGAAAC-3` and a reverse primer with the sequence 5`-AATTAAGCAGACAAATCACT-3`. Denaturation was completed by heating the reaction at 95ºC for 30 s. Annealing was carried out at 50ºC for 30 s. Polymerization was catalyzed by PFU at 72ºC for 1 min. The cycle was repeated 30 times. The PCR product was sequenced by the Ohio State Unversity Plant-Microbe Genomics Facility. Alignment was analyzed using BLAST technology (34).

N-terminal Serine Labeling

Label Introduction

To convert the N-terminal serine into aldehyde, the protein (resuspended in 100 mM phosphate buffer pH 6) was incubated with 5 mM $NaIO_4$ in for 15 minutes at 4°C. Excess periodate was then quenched by incubating with 15 mM glycerol for 15 min at 37°C. Buffer exchange was performed on the reaction using the same phosphate buffer to remove the glyceraldehyde product which would interfere with the labeling. To label the aldehyde-containing protein, 5 mM biotinamidohexanoic acid hydrazide or 1 mM fluorescein-5-thiosemicarbazide was added. The reaction was allowed to nutate overnight at 4°C (26, 27).

Reduction of Linkage

To reduce, $NaBH_4$ was added to a final concentration of 50 mM (in 100 mM phosphate buffer pH 6) and the reaction was incubated on ice overnight. The reaction should not be capped because the borohydride will produce low amounts of hydrogen gas in water. To ensure quenching of the borohydride, 1M HCl was added until bubbles subsided. The reaction was then dialyzed into water overnight at 4°C. Extent of ligation and reduction were analyzed by MALDI-TOF mass spectrometry (43).

Recombinant and Semisynthetic Histones

Fmoc Synthesis and Purification

The C-terminal region of H4 (AKRKTVTAMDVVYALK(ac)RQGRTLYGFGG) was synthesized using standard Fmoc protection strategies, using 2-(6-Chloro-1H-benzotriazole-1-yl)- 1,1,3,3-tetramethylaminium hexafluorophosphate (HCTU) and diisopropylethylamine (DIEA) activation on pre-loaded Gly-Wang resin (Novabiochem) (44). Synthesis was performed on an Aapptec Apex 396 synthesizer. The N-terminal alanine was coupled as a Boc-thiazolidine residue, in order to protect the cysteine during synthesis. Acetyl-lysine, as Fmoc-Lys(Ac)-OH, and Fmoc-Lys(Alloc)-OH were purchased from Novabiochem and coupled normally. Alloc deprotection was done by swelling resin in CH_2Cl_2, and adding phenylsilane (20 eq) and tetrakis(triphenylphosphine) palladium (0.35 eq) and nutating 30 minutes. Nbz conversion was performed by swelling resin in CH_2Cl_2, and adding p-nitrophenyl chloroformate (5 eq) followed by nutation for 45 minutes. Resin is then washed into dimethylformamide (DMF) and rinsed with 0.5 M DIEA for 15 minutes (45). Peptides were cleaved from the resin by nutating at 25ºC for 3 h in 94% TFA, 2.5% ethanedithiol, 2.5% H_2O, and 1% triisopropylsilane. After completion,

the cleavage solution was collected and concentrated under a nitrogen stream. The cleaved peptide was then precipitated with diethyl ether (10 eq), centrifuged, and separated from the supernatant. Thiazolidine ring opening to reveal the N-terminal cysteine was performed using 0.4M methoxylamine, 50mM HEPES pH 7.5 for 4 hours, and confirmed by analytical C18 RP-HPLC and MALDI-TOF mass spectrometry. The peptide was then purified using C18 RP-HPLC, using a gradient of Buffer B (90% acetonitrile and 0.1% trifluoroacetic acid (TFA) in water) in Buffer A (0.1% TFA in water). Pure pools were assessed by MALDI-TOF mass spectrometry and analytical C18 RP-HPLC. Pure samples were then lyophilized to dryness.

Thioester Expression

The truncated H4(1-75) was cloned into the pTXB1 plasmid and fused to the *Mxe* GyrA intein-Chitin Binding domain using standard cloning techniques. The plasmid was then transformed into *E.coli* BL21 (DE3) competent cells. Protein was overexpressed at 37ºC in LB media with 0.1 mg/mL ampicillin and induced at OD_{600} = 0.4 by addition of isopropyl β-D-1-thiogalactopyranoside (IPTG) to 1 mM final concentration for 3 h before harvesting by centrifugation (17).

Extraction from Inclusion Bodies

Cells were resuspended in 10 – 25 mL lysis buffer (25 mM HEPES pH 7.5, 1 mM EDTA, 1M NaCl, 1 mM PMSF) and lysed by sonication. After centrifucation at 20,000*g* for 15 min at 4 ºC, the thioester-containing pellet was separated from the supernatant. The pellet was washed twice in 25 mL of Triton wash buffer 25 mM HEPES pH 7.5, 1 mM EDTA, 1 M NaCl, 1% Triton X-100). The mixture was shaken for 20 min then centrifuged at 10,000*g* for 10 min at 4ºC and the supernatant was discarded. The pellet was washed in the same way in 25 mL of wash buffer

(Triton wash buffer without Triton X-100). DMSO (250 µL) was added to the pellet which was then minced with a spatula. This mixture was allowed to soak at 25 ºC for 30 min. The pellet was shaken in 30 mL of HU-500 buffer (6M urea, 25 mM HEPES pH 7.5, 1 mM EDTA, 500 mM NaCl) for 1 h to extract histones from the pellet then centrifuged at 15,000*g* for 10 min at 25 ºC. The supernatant was saved. This step was repeated without the DMSO soak. Extent of expression and extraction from inclusion bodies was evaluated by SDS-PAGE. Fractions containing thioester were pooled and either dialyzed against HU-100 (HU-500 with 100 mM NaCl) or diluted with HU-0 to reach 100 mM NaCl (17).

Thioester Purification

The dialyzed extract was purified by ion exchange over an SP-FF column (GE) by performing a gradient from HU-300 to HU-1000. Purified proteins were then refolded by dialysis into high salt buffer (25 mM HEPES pH 7.5, 1 mM EDTA, 1 M NaCl). Thiolysis was initiated by addition of 100 mM 2-mercaptoethane sulfonate (MESNA), and allowed to cleave overnight at 4°C. After cleavage, buffer components were adjusted to ligation conditions (6 M urea, 25 mM HEPES pH 7.5, 1 M NaCl, 1 mM EDTA, 50 mM MESNA) and then concentrated. The extent of cleavage was analyzed by SDS-PAGE (17).

Ligation

Purified thioester was first treated with 5mM tris(2-carboxyethyl)phosphine (TCEP), and then used to resuspend 2.2 molar equivalents of pure C-terminal modified peptide. After each addition pH was checked using pH strips. Ligation was allowed to proceed until complete as measured by SDS-PAGE gels. Ligation was generally completed after 8 hours. When ligation was completed, the sample was desulfurized to convert the cysteine residue at the ligation site

into the native alanine. An equivalent volume of 6M guanidine-HCl, 50mM HEPES pH 7.5, and 800mM TCEP was added to the sample which was then sparged with argon for 30 min. Reaction was initiated by the addition of VA-044US to 10mM and incubation at 42°C for 4 hours. Extent of desulfurization was determined by MALDI-TOF mass spectrometry. The sample was then purified using RP-HPLC, and pure samples were determined by MALDI-TOF mass spectrometry and SDS-PAGE. Pure pools were then lyophilized to dryness (17).

Recombinant Histone Expression and Purification

Wild-type recombinant histones from *Homo sapiens* were expressed and purified as previously described for thioesters through ion exchange chromatography. After this purification step, histone proteins were further purified by RP-HPLC. Pure samples were determined by MALDI-TOF spectrometry and pure pools were lyophilized to dryness. H3C110A, H4-K91Q, H2A-K119C, and H2A.Z I118C point mutations were created by site-directed mutagenesis (Stratagene) (17).

Histone Refolding

For the refolding of histones, tetramers made up of H3C110A and WT H4, H4-K91ac, or H4-K91Q, and dimers made up of H2A(K119C)-Flourescein and H2B or H2A.Z(I118C)-TAMRA and H_2B were mixed in equal molar ratios. The histones were dissolved in 6M Gdn-HCl, 25mM Tris pH 7.5, 1mM EDTA, and placed into engineered dialysis membranes and double dialyzed into 2M NaCl, 25mM Tris pH 7.5, 1mM EDTA. Refoldings were then purified by size-exclusion chromatography using a Superdex 200 10/300 GL column (GE Healthcare) using 2M NaCl, 25mM Tris pH 7.5, 1mM EDTA. The labeling of histones was done as previously described. Briefly, unfolded protein was resuspended in denaturing buffer at neutral pH and

purged under argon atmosphere. It was then incubated in the presence of TCEP to ensure that the cysteines were in a reduced state. Maleimide label, in dimethylformamide, was added dropwise until a final concentration of about 20 equivalents was reached. The reaction was allowed to proceed for 5h at 25°C and then quenched with DTT (5). For refoldings that are to be labeled by the aldehyde conversion, the Tris buffer is replaced with 50mM sodium phosphate pH 6.0.

Reconstitution and Sucrose Gradient Purification

DNA Constructs

For the high affinity nucleosome positioning 601 sequence (46), the following primers were used, 5'CTGGAGSSTCCCGGTGCCGAGGC that contained a Cy5 flourescent label for tracer DNA and did not for bulk DNA, and 5'ACAGGATGTATATATCTGACACGTGCC. All PCRs were purified by HPLC using a Gen-Pak Fax column (Waters) and a gradient from TE-0 (20 mM Tris pH 7.5, 1 mM EDTA) to TE-1000 (20 mM Tris pH 7.5, 1 mM EDTA, 1 M NaCl).

Reconstitution

Purified tetramers, dimers, and DNA were mixed at a 1:2.2:1.1 molar ratio, unless otherwise noted, and dialyzed using engineered dialysis membranes into 25mM Tris pH 7.5, 1mM EDTA (47). These nucleosomes were then sucrose purified using a 5-35% sucrose gradient, spun at 288,000g for 22 hours. Fractions were analyzed by Native-PAGE. Gels were scanned on a Typhoon Imager (GE) and quantitation was done in ImageQuant. Pools were then concentrated, and concentration was determined by Nanospec UV absorbance at 280nm.

REFERENCES

1. Andrews AJ, Luger K. Nucleosome structure(s) and stability: variations on a theme. Annu Rev Biophys. 2011;40:99-117.
2. Mersfelder EL, Parthun MR. The tale beyond the tail: histone core domain modifications and the regulation of chromatin structure. Nucleic Acids Res. 2006;34(9):2653-62. PMCID: 1464108.
3. Simon M, North JA, Shimko JC, Forties RA, Ferdinand MB, Manohar M, et al. Histone fold modifications control nucleosome unwrapping and disassembly. Proc Natl Acad Sci U S A. 2011;108(31):12711-6. PMCID: 3150920.
4. Manohar M, Mooney AM, North JA, Nakkula RJ, Picking JW, Edon A, et al. Acetylation of histone H3 at the nucleosome dyad alters DNA-histone binding. J Biol Chem. 2009;284(35):23312-21. PMCID: 2749105.
5. Shimko JC, North JA, Bruns AN, Poirier MG, Ottesen JJ. Preparation of fully synthetic histone H3 reveals that acetyl-lysine 56 facilitates protein binding within nucleosomes. J Mol Biol. 2011;408(2):187-204. PMCID: 3815667.
6. Jenuwein T, Allis CD. Translating the histone code. Science. 2001;293(5532):1074-80.
7. Ye J, Ai X, Eugeni EE, Zhang L, Carpenter LR, Jelinek MA, et al. Histone H4 lysine 91 acetylation a core domain modification associated with chromatin assembly. Mol Cell. 2005;18(1):123-30. PMCID: 2855496.
8. Guo J, Wang J, Lee JS, Schultz PG. Site-specific incorporation of methyl- and acetyl-lysine analogues into recombinant proteins. Angew Chem Int Ed Engl. 2008;47(34):6399-401.
9. Yan Q, Dutt S, Xu R, Graves K, Juszczynski P, Manis JP, et al. BBAP monoubiquitylates histone H4 at lysine 91 and selectively modulates the DNA damage response. Mol Cell. 2009;36(1):110-20. PMCID: 2913878.
10. Marmorstein R, Trievel RC. Histone modifying enzymes: structures, mechanisms, and specificities. Biochim Biophys Acta. 2009;1789(1):58-68. PMCID: 4059211.
11. Chatterjee A, Guo J, Lee HS, Schultz PG. A genetically encoded fluorescent probe in mammalian cells. J Am Chem Soc. 2013;135(34):12540-3. PMCID: 3783214.
12. Niu W, Schultz PG, Guo J. An expanded genetic code in mammalian cells with a functional quadruplet codon. ACS Chem Biol. 2013;8(7):1640-5.
13. Huang Y, Russell WK, Wan W, Pai PJ, Russell DH, Liu W. A convenient method for genetic incorporation of multiple noncanonical amino acids into one protein in Escherichia coli. Mol Biosyst. 2010;6(4):683-6.
14. Xiao H, Peters FB, Yang PY, Reed S, Chittuluru JR, Schultz PG. Genetic incorporation of histidine derivatives using an engineered pyrrolysyl-tRNA synthetase. ACS Chem Biol. 2014;9(5):1092-6. PMCID: 4033645.
15. Masumoto H, Hawke D, Kobayashi R, Verreault A. A role for cell-cycle-regulated histone H3 lysine 56 acetylation in the DNA damage response. Nature. 2005;436(7048):294-8.
16. Muir TW. Semisynthesis of proteins by expressed protein ligation. Annu Rev Biochem. 2003;72:249-89.
17. Shimko JC, Howard CJ, Poirier MG, Ottesen JJ. Preparing semisynthetic and fully synthetic histones h3 and h4 to modify the nucleosome core. Methods Mol Biol. 2013;981:177-92. PMCID: 3815671.
18. Wan Q, Danishefsky SJ. Free-radical-based, specific desulfurization of cysteine: a powerful advance in the synthesis of polypeptides and glycopolypeptides. Angew Chem Int Ed Engl. 2007;46(48):9248-52.
19. Siman P, Karthikeyan SV, Brik A. Native chemical ligation at glutamine. Org Lett. 2012;14(6):1520-3.

20. Haase C, Rohde H, Seitz O. Native chemical ligation at valine. Angew Chem Int Ed Engl. 2008;47(36):6807-10.
21. Harpaz Z, Siman P, Kumar KS, Brik A. Protein synthesis assisted by native chemical ligation at leucine. Chembiochem. 2010;11(9):1232-5.
22. Townsend SD, Tan Z, Dong S, Shang S, Brailsford JA, Danishefsky SJ. Advances in proline ligation. J Am Chem Soc. 2012;134(8):3912-6. PMCID: 3306728.
23. Oppenheim A, Katzir N. Advancing the onset of mitosis by cell free preparations of Physarum polycephalum. Exp Cell Res. 1971;68(1):224-6.
24. Thiriet C, Hayes JJ. Histone proteins in vivo: cell-cycle-dependent physiological effects of exogenous linker histones incorporated into Physarum polycephalum. Methods. 1999;17(2):140-50.
25. Richard JP, Melikov K, Vives E, Ramos C, Verbeure B, Gait MJ, et al. Cell-penetrating peptides. A reevaluation of the mechanism of cellular uptake. J Biol Chem. 2003;278(1):585-90.
26. Atha DH, Brew SA, Ingham KC. Interaction and thermal stability of fluorescent labeled derivatives of thrombin and antithrombin III. Biochim Biophys Acta. 1984;785(1-2):1-6.
27. Wendeler M, Grinberg L, Wang X, Dawson PE, Baca M. Enhanced catalysis of oxime-based bioconjugations by substituted anilines. Bioconjug Chem. 2014;25(1):93-101.
28. Prior CP, Cantor CR, Johnson EM, Allfrey VG. Incorporation of exogenous pyrene-labeled histone into Physarum chromatin: a system for studying changes in nucleosomes assembled in vivo. Cell. 1980;20(3):597-608.
29. Mohberg J, Rusch HP. Growth of large plasmodia of the myxomycete Physarum polycephalum. J Bacteriol. 1969;97(3):1411-8. PMCID: 249862.
30. Guttes E, Guttes S, Rusch HP. Morphological observations on growth and differentation of Physarum polycephalum grown in pure culture. Dev Biol. 1961;3:588-614.
31. Thiriet C, Hayes JJ. A novel labeling technique reveals a function for histone H2A/H2B dimer tail domains in chromatin assembly in vivo. Genes Dev. 2001;15(16):2048-53. PMCID: 312765.
32. Elliott GO, Murphy KJ, Hayes JJ, Thiriet C. Replication-independent nucleosome exchange is enhanced by local and specific acetylation of histone H4. Nucleic Acids Res. 2013;41(4):2228-38. PMCID: 3575802.
33. Bailey LM, Ivanov RA, Wallace JC, Polyak SW. Artifactual detection of biotin on histones by streptavidin. Anal Biochem. 2008;373(1):71-7.
34. Gargas A, Taylor, J.W. Polymerase Chain Reaction (PCR) Primers for Amplifying and Sequencing Nuclear 18s rDNA from Lichenized Fungi. Mycologia. 1992;84(4):589-92.
35. Karimi K, Zamani A. Mucor indicus: biology and industrial application perspectives: a review. Biotechnol Adv. 2013;31(4):466-81.
36. Almeida CA, de Campos-Takaki GM, Portela MB, Travassos LR, Alviano CS, Alviano DS. Sialoglycoproteins in morphological distinct stages of Mucor polymorphosporus and their influence on phagocytosis by human blood phagocytes. Mycopathologia. 2013;176(3-4):183-9.
37. Rosenbluh J, Singh SK, Gafni Y, Graessmann A, Loyter A. Non-endocytic penetration of core histones into petunia protoplasts and cultured cells: a novel mechanism for the introduction of macromolecules into plant cells. Biochim Biophys Acta. 2004;1664(2):230-40.
38. Ryser HJ, Hancock R. Histones and basic polyamino acids stimulate the uptake of albumin by tumor cells in culture. Science. 1965;150(3695):501-3.
39. Hariton-Gazal E, Rosenbluh J, Graessmann A, Gilon C, Loyter A. Direct translocation of histone molecules across cell membranes. J Cell Sci. 2003;116(Pt 22):4577-86.
40. Thiriet C. Analysis of chromatin assembled in vivo using exogenous histones in Physarum polycephalum. Methods. 2004;33(1):86-92.

41. Turck N, Richert S, Gendry P, Stutzmann J, Kedinger M, Leize E, et al. Proteomic analysis of nuclear proteins from proliferative and differentiated human colonic intestinal epithelial cells. Proteomics. 2004;4(1):93-105.
42. Kuroishi T, Rios-Avila L, Pestinger V, Wijeratne SS, Zempleni J. Biotinylation is a natural, albeit rare, modification of human histones. Mol Genet Metab. 2011;104(4):537-45. PMCID: 3224183.
43. Fukuda M. Chemical labeling of carbohydrates by oxidation and sodium borohydride reduction. Curr Protoc Mol Biol. 2001;Chapter 17:Unit17 5.
44. North JA, Shimko JC, Javaid S, Mooney AM, Shoffner MA, Rose SD, et al. Regulation of the nucleosome unwrapping rate controls DNA accessibility. Nucleic Acids Res. 2012;40(20):10215-27. PMCID: 3488218.
45. Mahto SK, Howard CJ, Shimko JC, Ottesen JJ. A reversible protection strategy to improve Fmoc-SPPS of peptide thioesters by the N-Acylurea approach. Chembiochem. 2011;12(16):2488-94. PMCID: 3558277.
46. Lowary PT, Widom J. New DNA sequence rules for high affinity binding to histone octamer and sequence-directed nucleosome positioning. J Mol Biol. 1998;276(1):19-42.
47. Thastrom A, Lowary PT, Widom J. Measurement of histone-DNA interaction free energy in nucleosomes. Methods. 2004;33(1):33-44.